RPU-S47

RADIO PROPAGATION UNIT

Scientific Report No 47

PHOTOCHEMISTRY OF OZONE

By

A. P. Mitra

May 31 1969

NATIONAL PHYSICAL LABORATORY, DELHI - 12, INDIA

PHOTOCHEMISTRY OF OZONE

By

A. P. Mitra

National Physical Laboratory, New Delhi-12, INDIA*

Abstract

Photochemical calculations on mesospheric ozone are reviewed for oxygen only, oxygen-hydrogen and oxygen-hydrogen-nitrogen atmospheres. Effects of vertical eddy transport included in recent works by Hesstvedt (1968) and by Shimazaki (1968) are discussed.

The close relation that exists between the ratio $n(O)/n(O_3)$ and negative ion and electron concentrations brings in a new dimension in ozone photochemistry work. A remarkable similarity has been observed by Doherty between LF phase variations during a solar eclipse and the computed variations in ozone concentrations. Similarities also exist during sunrise and sunset. It thus seems possible to obtain synoptic information on mesospheric ozone from Ionospheric parameters.

---

* Part of this work was done at Goddard Space Flight Center, Greenbelt, Md., U.S.A. where the author was spending a year's leave of absence as an NRC-NASA Senior Research Associate.

Introduction

The few rocket measurements of ozone concentrations in the mesosphere summarised in Fig.1, form the basis against which photochemical theories must be judged. The main features of these measurements, available generally upto about 70 Km, are a monotonic decrease of ozone concentration in day-time and larger values at night with a mesospheric maximum. In some recent Japanese experiments, a daytime maximum has also been observed at mesoppheric heights, Typical daytime values are : $5 \times 10^{11} cm^{-3}$ at 40 Km, $5 \times 10^{10} cm^{-3}$ at 50 Km, $8 \times 10^{9} cm^{-3}$ at 60 Km and $6 \times 10^{8} cm^{-3}$ at 70 Km (Johnson et al, 1952).

Photochemical theories of ozone date from the pioneering work of Chapman (1930) in which reactions revolving O, O_3, O_2 were only considered. This scheme is now known to be over simplified and gives an excess of ozone in the mesosphere. Following the identification of the Meinel bands of airglow with OH, the importance of hydrogen-oxygen reactions was recognized, resulting in the first major work on the photochemistry of water vapour by Bates and Nicolet (1950). The two ozone photochemistry works by Hunt followed - one on the time-dependent solutions of the oxygen-only situation (Hunt, 1965); and soon afterwards realising that the oxygen-only situation yielded a distribution considerably in excess of the rocket-measured profiles (the only one available then was by Johnson et al, 1956) followed with a second work (Hunt, 1966) using a complex hydrogen-oxygen reaction scheme. The result-

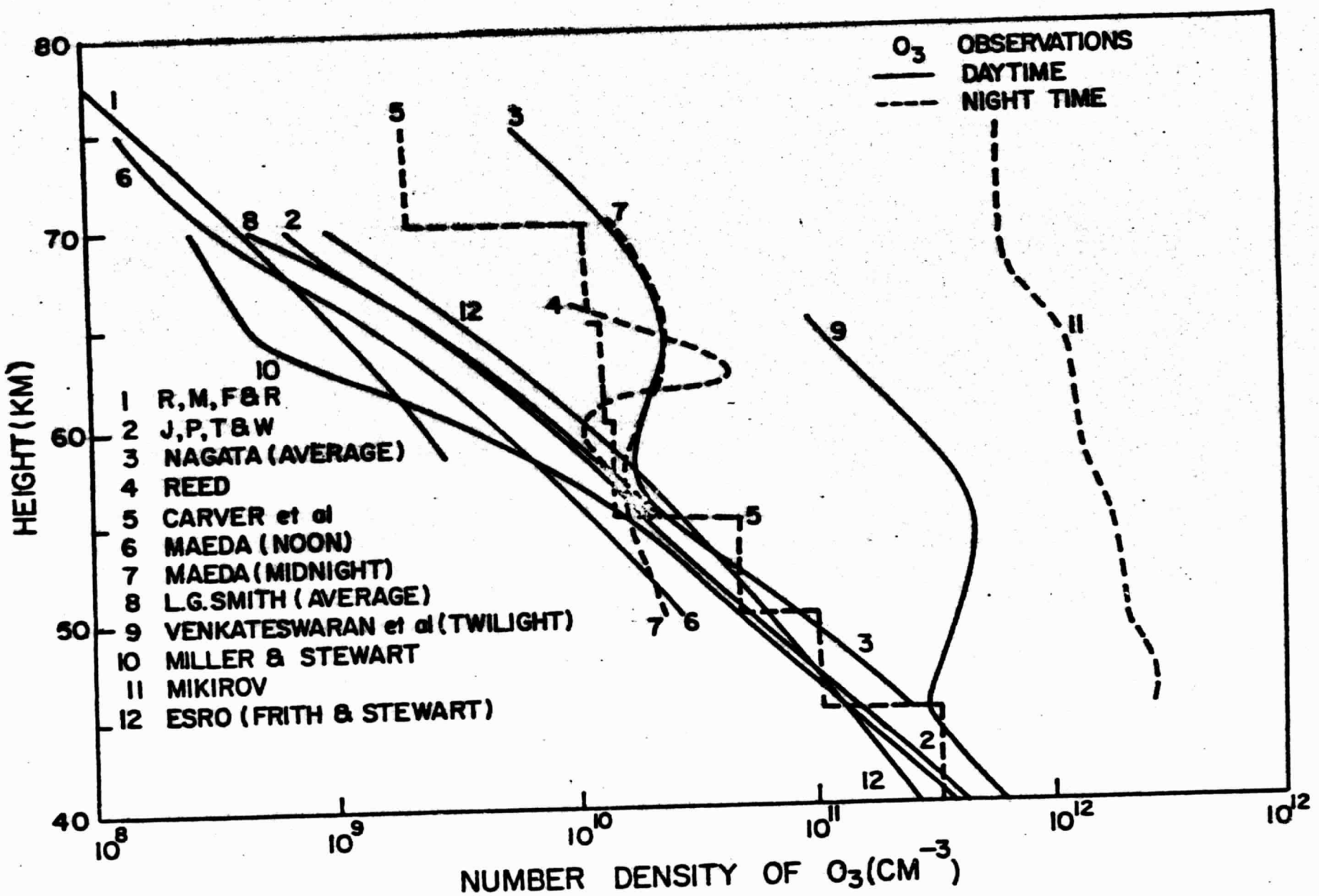

Legends of Diagrams

Fig.1 Observations on ozone distributions obtained by various workers with rocket and satellite-borne instruments.

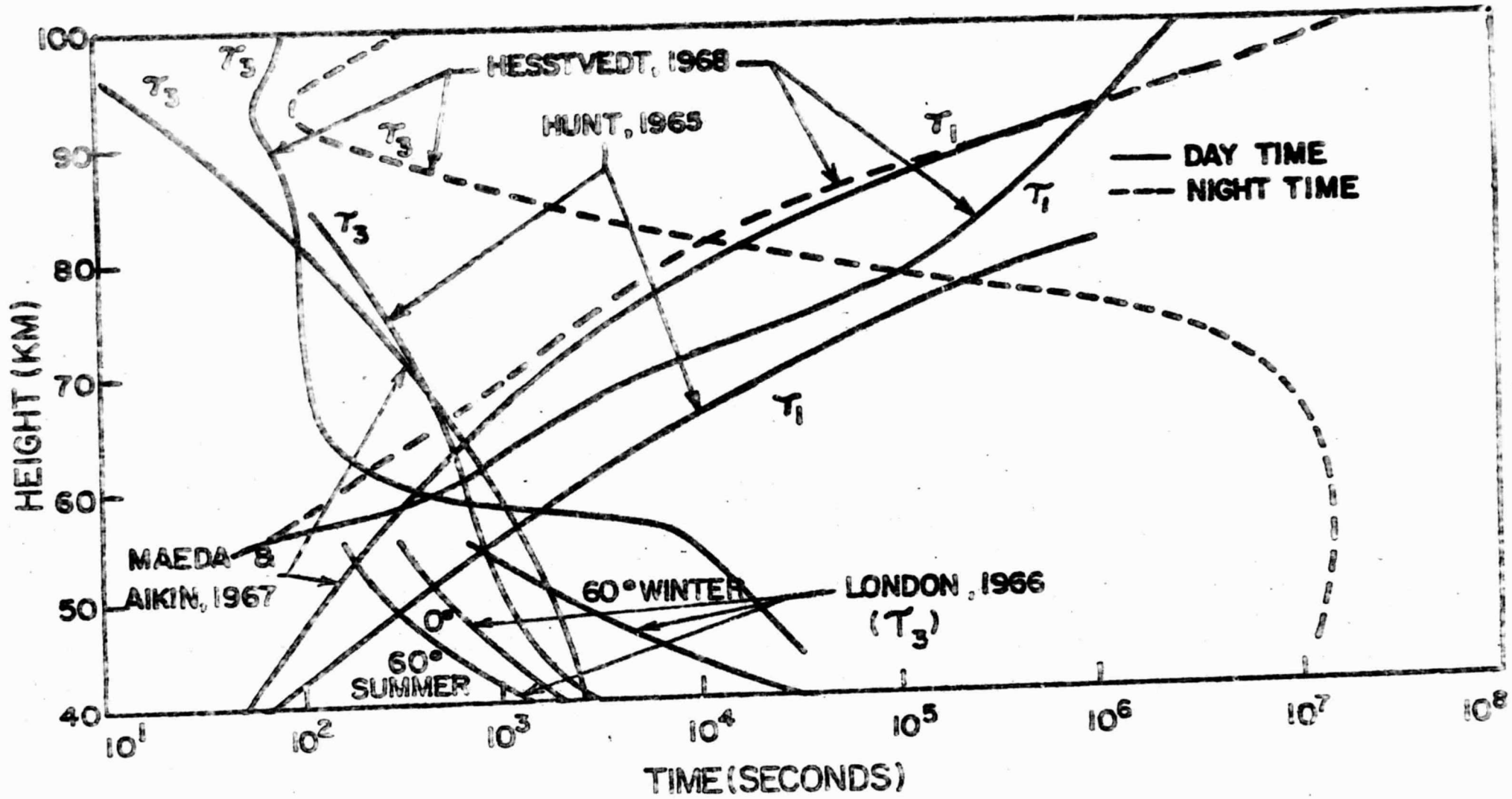

Fig.2 Characteristic times for atomic oxygen (τ_1) and ozone (τ_3) computed by different workers. Hesstvedt's curves include oxygen-hydrogen reactions; the others for oxygen-only atmosphere.

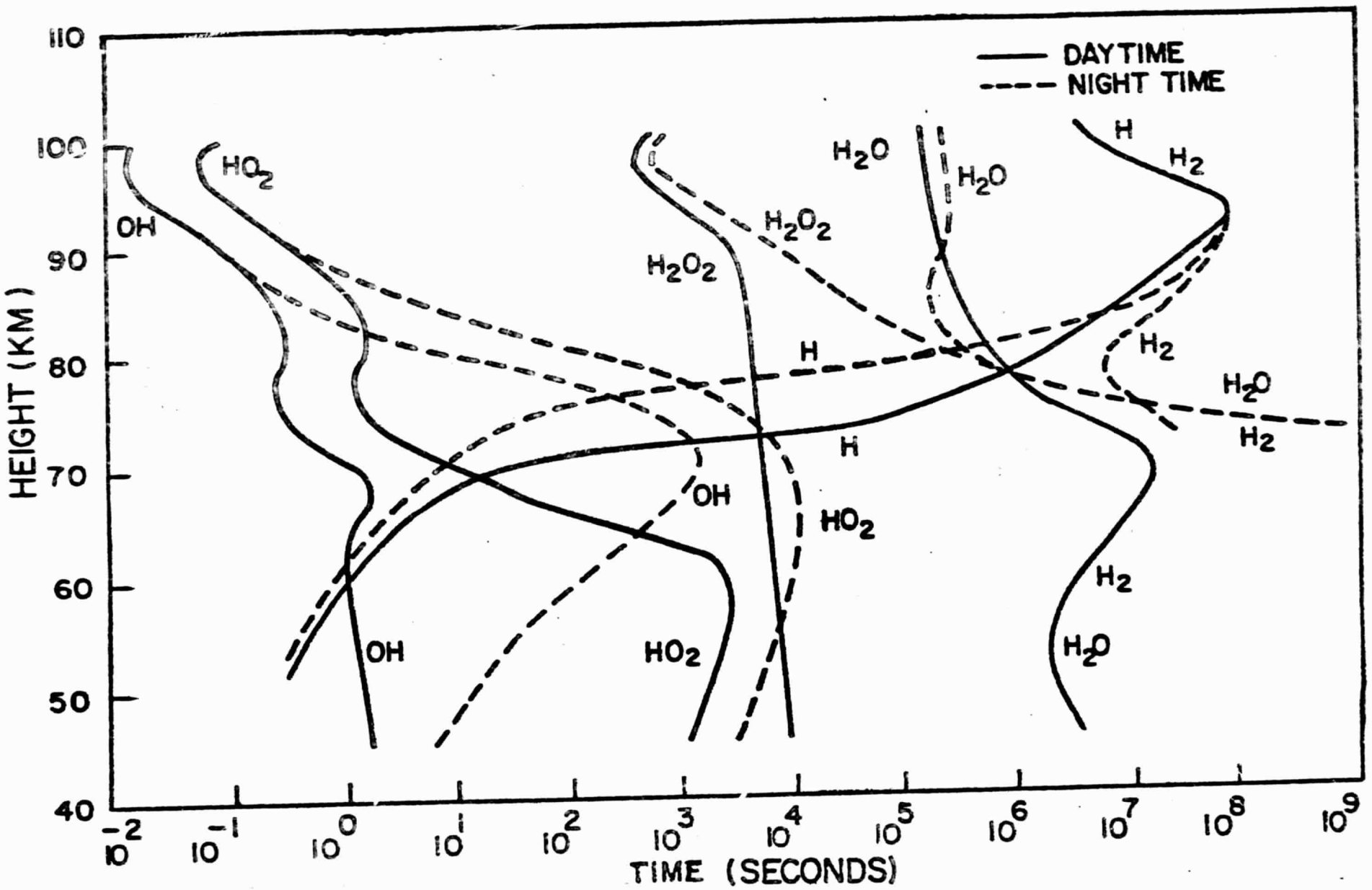

Fig.3 Characteristic times for water vapour and various hydrogen components.

ing agreement with rocket observations was better, although as we shall see later, this by itself is not very meaningful. The next development came with the realisation that in the region where the characteristic photochemical times are large (see, for example Fig.2) static models can have no meaning. One must then take into account any effect of atmospheric motions, either large-scale or small-scale (turbulence). This, and one might call the third phase in oxygen photochemistry, began with the work of Colegrove, Hanson and Johnson (1965) who brought in the concept of eddy diffusion and oxygen transport in the lower thermosphere in a calculation combining some recent measurements of the O/O_2 concentration ratio above 120 Km with the then available knowledge of dissociation, recombination and molecular diffusion rates. Subsequent works in this line was carried out by Shimazaki (1967, 1968) whose most recent work with Laird (private communication) considers the effects of eddy diffusion processes on the height distributions of 14 components of the oxygen-hydrogen-nitrogen atmosphere. In an important recent work, Hesstwedt (1968) obtained new distribution for $O(^3P)$ and O_3 for eddy diffusion coefficients varying from $4 \times 10^5 cm^2/s$ at 65 Km to $7 \times 10^6 cm^2/s$ at 100 Km and with photochemical values taken as the boundary conditions. He found the most striking ratios in the mixing ratios of the major hydrogen components H_1 H_2 and H_2O and a substantial depletion of both O and O_3 near the mesosphere - a result of great significance in negative ion chemistry.

The fourth phase of ozone photochemistry that has just began to emerge is the very close relationship that exists between ozone concentration and mesospheric ionization, and the possibility of obtaining information on ozone variations from D region parameters. An important work in this area is by Doherty (1968) who noticed a remarkable similarity between changes in phase of a low frequency radio wave during a solar eclipse and Hunt's computed ozone variations. Reactions have been identified in the laboratory, and their rates have been measured, relating a number of negative ions with either O and O_3, with important consequences in the ozone theory.

In this work the four phases of oxygen photochemistry are outlined.

2. Oxygen-only Atmosphere

The oxygen-only atmosphere, first outlined by Chapman (1930), consists of the following reactions :

$$O_2 + h\nu \xrightarrow{\lambda < 2424\ \text{Å}} O + O \qquad (J_2)$$

$$O_3 + h\nu \xrightarrow{\lambda < 11{,}800\text{Å}} O + O_3 \qquad (J_3)$$

$$O + O + M \longrightarrow O_2 + M \qquad (k_{11})$$

$$O + O_2 + M \longrightarrow O_3 + M \qquad (k_{12})$$

$$O + O_3 \longrightarrow 2O_2 \qquad (k_{13})$$

for which the relevant reaction rates have the following values :

(i) $k_{11} \simeq 2.7 \times 10^{-33} \text{cm}^6/\text{s}$ Reeves et al (1960)

$$\simeq 3 \times 10^{-33} \left(\frac{T}{300}\right)^{-2.3 \pm 0.4}$$

(ii) k_{12} $8 \times 10^{-35} \exp(\frac{445}{T})$ cm^6/s Benson and Axworthy (1965)

* $(5.5 \pm 2) \times 10^{-34} \left(\frac{T}{300}\right)^{-2.5 \pm 0.3}$ cm^6/s

(iii) k_{13} $5.6 \times 10^{-11} \exp\left(-\frac{2650}{T}\right)$ Benson and Axworthy (1965)

* $(1.4 \pm 0.3) \times 10^{-12} \exp\left(-\frac{1500 \pm 200}{T}\right)$.

Those marked with asterisks are more recent values.

The time rate of change of O and O_3 in this simple scheme are given by :

$$\frac{dn(O)}{dt} = 2J_2 n(O_2) + J_3 n(O_3) - 2k_{11} n^2(O) n(M) - k_{12} n(O) n(O_2) - k_{13} n(O) n(O_3) \quad (1)$$

$$\frac{dn(O_3)}{dt} = k_{12} n(O) n(O_2) n(M) - J_3 n(O_3) - k_{13} n(O) n(O_3) n(M) \quad (2)$$

Under equilibrium condition, ozone and atomic oxygen concentrations are simply related by :

$$\frac{n(O_3)}{n(O)} = \frac{k_{12} n(O_2) n(M)}{J_3 + k_{13} n(O) n(O_3) n(M)} \quad (3)$$

and if k_{13} is really as low as that given above the ratio for all heights above 60 Km is given by

$$\frac{n(O_3)}{n(O)} \simeq 10^{-31} \left(\frac{T}{300}\right)^{-2.5} n(O_2) n(M) \quad (4)$$

An important parameter is the characteristic time (half-restoration time) which determines if and when photochemical equilibrium can be established. These are the times taken for departures $\Delta n(O)$ or $\Delta n(O_3)$ from the equilibrium values $n(O)$ and $n_o(O_3)$ to be reduced to e^{-1} of their initial values. The following expressions for the characteristic times may be derived (Dutsch, 1956) :

$$\tau_3 = k_{12}n(O_2)n(M)/4J_3k_{13}n_e(O_3) \qquad (5)$$

$$\tau_1 = \frac{J_3}{2J_2k_{13}n(O_2)-4k_{12}k_{13}n(O_2)n(M)n_o(O)}$$

The characteristic times for O and O_3 as calculated by Hunt (1965) on the above basis and by Maeda and Aikin from a time dependent study of the equations (1) and (2), are given in Fig. 2. Characteristic times for an oxygen-hydrogen atmosphere, calculated under the condition of photochemical equilibrium, are also shown; there are two sets of the latter values, one given by Hunt (1966) and the other by Nesstvedt (1968). While there are some differences in the times given by the various authors, the basic conclusion is the same; namely that the characteristic time for ozone for the daytime mesosphere is short-from a few minutes to a fraction of an hour - and consequently Eq. (3), valid for photochemical equilibrium, can be used. In the troposphere and the stratosphere, however, the characteristic times for atomic oxygen is short at 40 Km, but is large and increases rapidly with height in the mesosphere, so that transport must play a very dominant part for this constituent. Typical values of the characteristic times during day are :

Characteristic Times

	τ_O (seconds)	τ_{O_3} (seconds)
40	10^2	3×10^3
60	10^3	10^3
80	10^5	10^2*
100	10^7	10^2

* Large at night when n(O) is small.

Hunt has calculated O-O_3 distribution with this simple case as well as for the oxygen-hydrogen atmosphere which we will discuss latter. The main difference, it appears, is that a pure oxygen atmosphere leads to an excess of ozone. The ozone distributions such as those given by Hunt and most recently by Maeda and Aikin (1967) must therefore be considered as very gross.

The main virtue, however, of these simple calculations is that these give a clue to the type of variations that one may expect with time or with latitude, or with seasonal changes in mesospheric temperature. Variation of ozone and atomic oxygen concentrations with time as calculated by Maeda and Aikin (1967) are shown in Fig. 4; and those with latitude as calculated by London are shown in Fig.5. The reaction rates used are identical in both, and are those marked (a) in Table 2. There is no diurnal variation in ozone at 50 Km (as one would expect from the large characteristic time at this altitude), but nighttime enhancements appear at greater heights. The nighttime distribution shows a maximum at about 70 Km in the Maeda-Aikin model as well as in the pure oxygen model of Hunt, but it

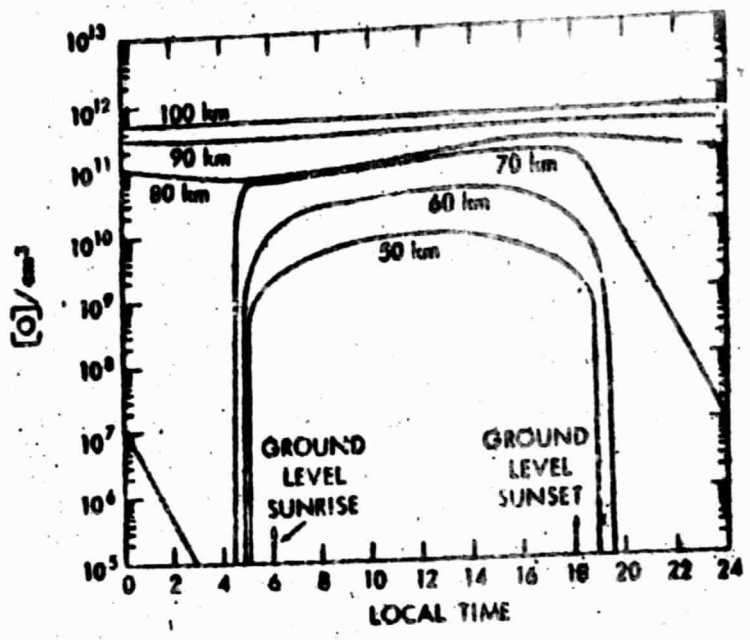

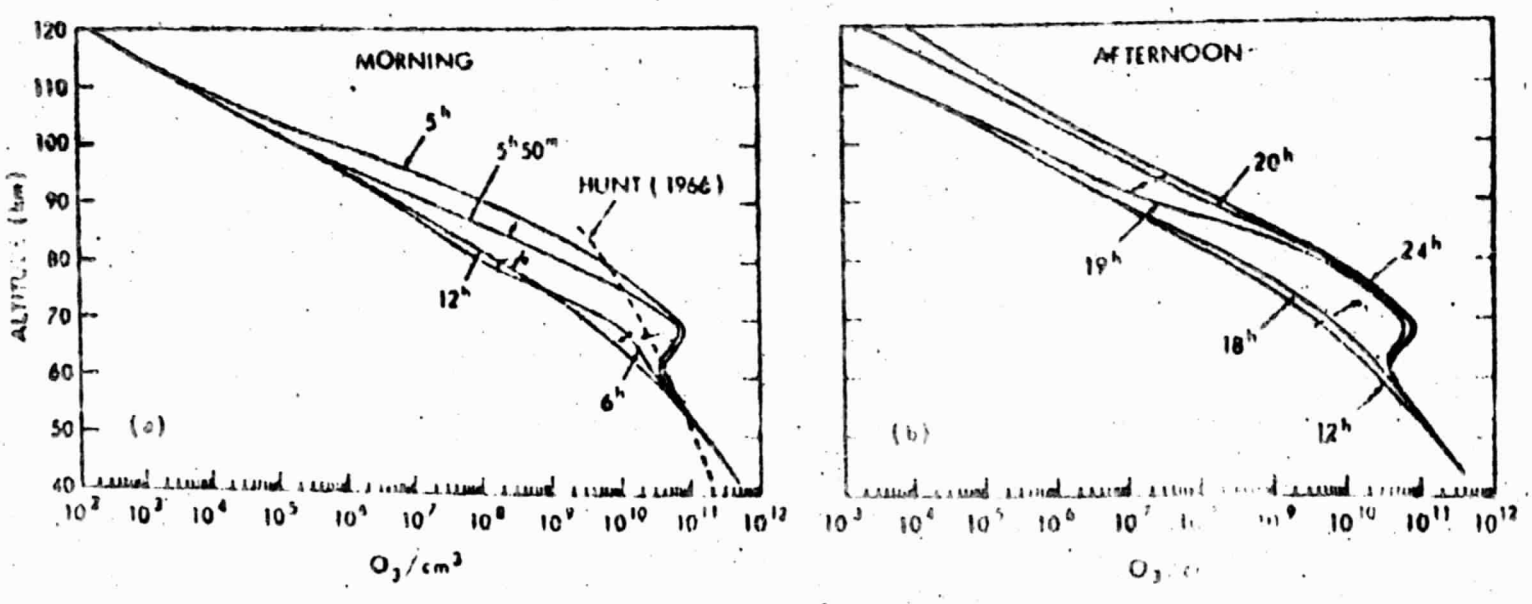

(a) Increasing phase.

(b) Decreasing phase.

Fig.4 Diurnal variations of atomic oxygen and ozone computed by Maeda and Aikin (1967) for an oxygen-only atmosphere.

OZONE DISTRIBUTIONS

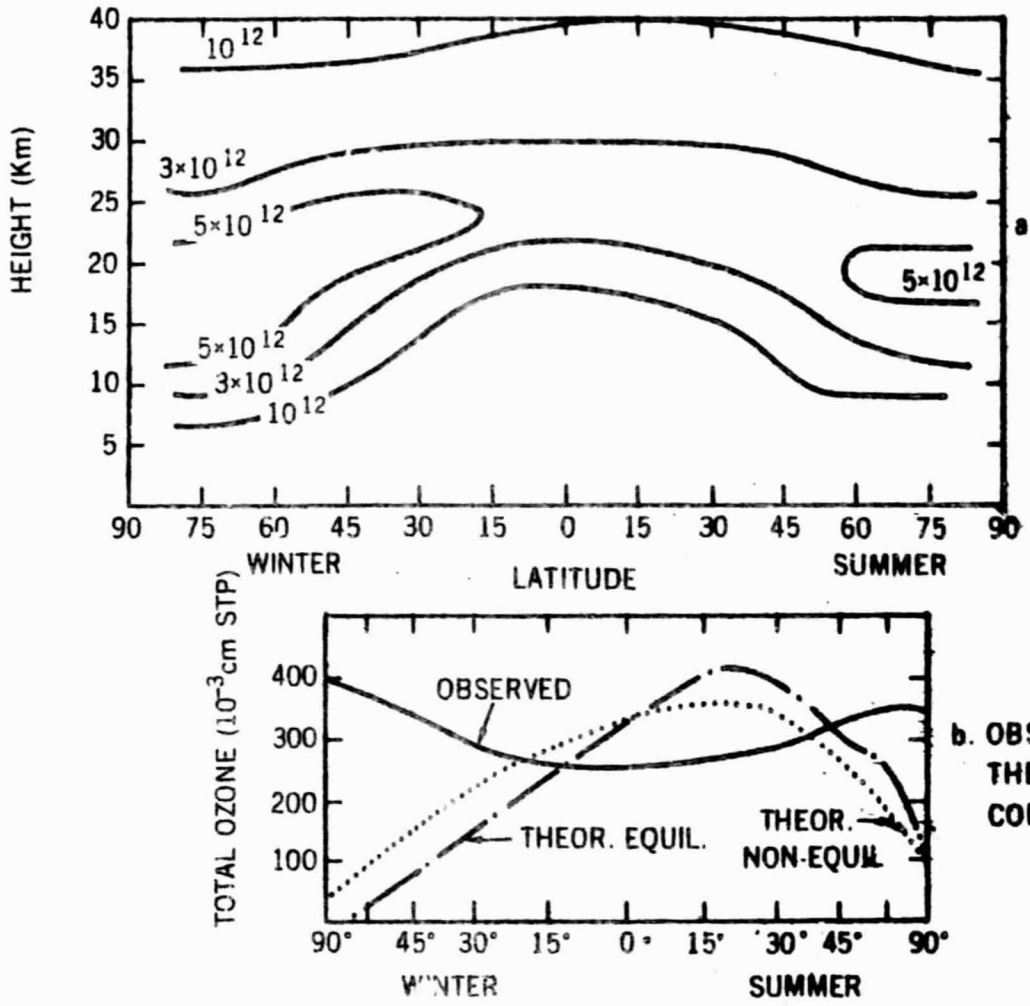

a. OBSERVED LATITUDE DISTRIBUTION

b. OBSERVED AND THEORETICAL COMPARISON

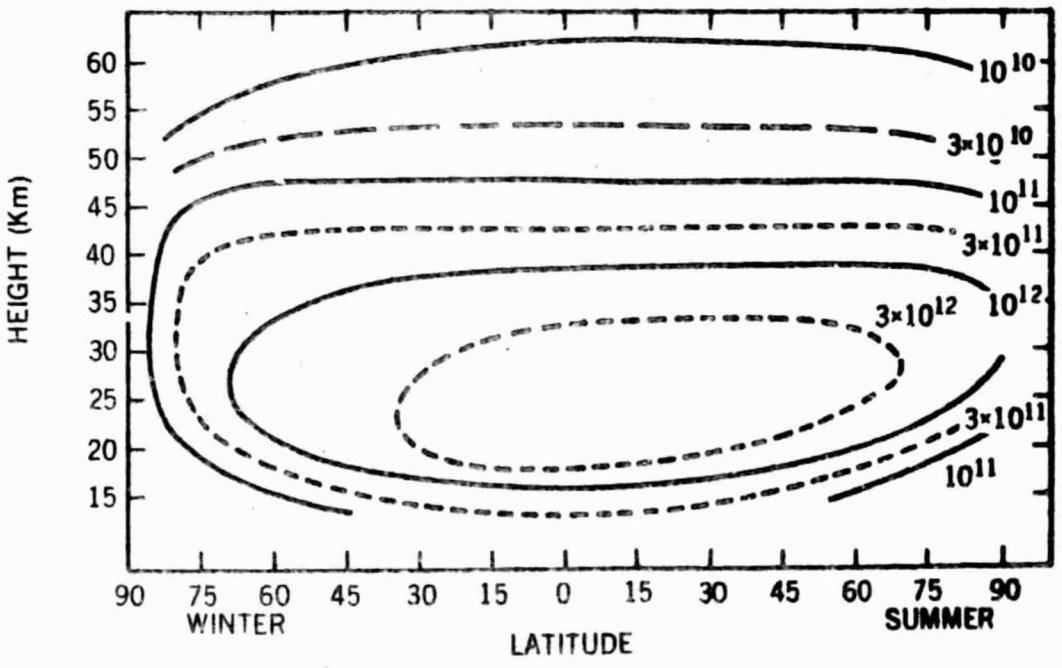

c. PHOTOCHEMD (NON-EQUILIBRIUM)

Fig.5 Latitude variations in ozone concentration computed by London (1967) compared with observational results.

Table 1. Photochemical Models of Ozone

Authors	Conditions	Remarks
Barth (1961)	Oxygen-Nitrogen Atmosphere Time Dependent solution	Considers nine reactions between M, O, O_2, O_3. NO and NO_2 Diurnal variation given
Hunt (1963)	Oxygen-only	Overhead sun
	Equilibrium case	Used $k_{13} = 6.45 \times 10^{-12} \exp\left(\frac{3300}{RT}\right)$ cm^3/s 1959 ARDC atmosphere
Hunt (1965)	Oxygen-only	Overhead sun
	Non-Equilibrium case.	1963 equilibrium values used as preliminary values. Assumed 5×10^{13} molecules/cm^2 column and 4.6×10^{19} molecules/cm^2 column for O_3 amount and O_2 amount above 80 Km respectively.
Hunt (1965)	Solar Eclipse with following particulars :	Air model and rate coefficients as in earlier models.
	i. Time of eclipse from first contact to fourth contact = 9000 seconds	No change in O_3 below 45 Km Substantial changes in O_3 in the mesosphere. Time curves given for 61.25 Km and 78.75 Km. Increase of less than 1% of the total O_3 amount expected, compared to experimental observations of 4 %
	ii. At instant of totability at 4000 seconds no solar radiation reached the earth.	
	Oxygen-only Atmosphere.	O concentration remains unchanged above 70 Km inspite of large O_3 increase.
Hunt (1966)	Oxygen-hydrogen atmosphere	28 Reactions used with rate coefficients taken largely from Kaufman (1964)

Authors	Conditions	Remarks
	Both Equilibrium and Non-equilibrium solutions.	Excess of ozone obtained under oxygen-only case largely removed, O_3 content decreasing from 0.9 to 0.2 cm STP (0.17 cm STP under non-equilibrium case).
Maeda and Aikin(1967)	Oxygen-only Both Equatorial and polar regions.	For polar atmosphere particle dissociation is assumed through process : $O_3 + O \quad O + O_2 + e$ E > 1 ev For equatorial atmosphere results similar to Hunt's between 50 to 80 Km, but above 80 Km, their O_3 concentrations less than Hunt's.
London (1967)	Oxygen-only Time-dependent solution	Derives latitudinal and seasonal variation. Uses Cole and Kantor distribution of pressure and temperature and the following rate coefficients : $k_{11} = 2.8 \times 10^{-33} cm^6 sec^{-1}$ $k_{12} = 2.0 \times 10^{-34} cm^3 sec^{-1}$ $k_{13} = 5.1 \times 10^{-10} \exp(-3000/T) cm^3 sec^{-1}$
Hesstvedt (1968 a)	Oxygen-hydrogen atmosphere 15-40 Km	Calculates O(1D), O(3P), O_3, OH, HO_2, H_2, H_2O, H_2O_2 and H.
	Also modification due to vertical eddy transport ($K_z = 4 \times 10^3 cm^2/s$	Reaction rates as in Hunt (1966) and Hesstvedt (1968b)
Hesstvedt (1968b)	Oxygen-hydrogen atmosphere with eddy diffusion 50 - 100 Km Eddy diffusion coefficient assumed to vary from $4 \times 10^5 cm^2$ at 65 Km to $7 \times 10^6 cm^2$ at 100 Km	O-distribution shows a broad maximum around 90-95 Km, and a pocket of low concentration around 80 Km. H_2O concentration considerably increased.
Shimazaki and Lavid (private Communication)	Oxygen-hydrogen-nitrogen atmosphere with eddy diffusion. Time-dependent solution.	Height distribution of 14 atmospheric components calculated : O(3P), O(1D), O_2, O_3, OH, H, HO_2, H_2O, H_2O_2, H_2, NO, NO_2, N, N_2O

Authors	Conditions	Remarks
	Three types of eddy diffusion coefficients assured : (a) a constant value of $10^6 cm^2 sec^{-1}$ (b) a constant value of $10^7 cm^2 sec^{-1}$ (c) coefficient varying linearly from $5 \times 10^5 cm^2 sec^{-1}$ at 40 Km to $5 \times 10^6 cm^2 sec^{-1}$ at 100 Km and constant at $5 \times 10^6 cm^2 sec^{-1}$ above 100 Km.	
Keneshea (1966)	Oxygen-Hydrogen-Nitrogen atmosphere, along with all major reactions involving positive and negative ions.	Using the computer code developed by Keneshea (1963), computes variations of several neutral species as well as those of major positive and negative ions during the solar eclipse of 12 November, 1966. Increase in ozone at mesospheric heights given as a function of time during eclipse.

TABLE 2

REACTIONS INVOLVED IN OZONE PHOTOCHEMISTRY (OXYGEN-HYDROGEN CASE)

REACTION	REACTION RATES cm^3/s(2 body); cm^6/s(3 body)	REMARKS
1. $O_2+h\nu \xrightarrow[\text{(Herzberg)}]{1750<\lambda<2424A} O(^3P)+O(^3P)$		1-3 are the main sources of production of O(3P). The dissociation rates are given by : $J = \int_{\lambda_1}^{\lambda_2} A_\lambda Q_{\infty\lambda} e^{-\tau_\lambda} d\lambda$ where A_λ is the absorption coefficient at wavelength λ, $Q_{\infty\lambda}$ is the number of dissociating photons outside the atmosphere at that wavelength and τ_λ is the optical depth.
2. $O_2+h\nu \xrightarrow[\text{(Schumann Runge)}]{\lambda<1750A} O(^1D)+O(^3P)$		
3. $O_3+h\nu \xrightarrow{3100<\lambda<11800A} O_2 + O(^3P)$		
4. $O_3+h\nu \xrightarrow[\text{(Hartley)}]{\lambda< 3100\ A} O_2 + O(^1D)$		
5. $O(^3P) + O_2+M \longrightarrow O_2 + M$	(a) $8\times10^{-35}\exp(890/RT)$ (b) $(5.5\pm2)\times10^{-34}\left(\frac{T}{300}\right)^{-2.5\pm0.3}$	5. The new value of (b) is
6. $O(^3P) + O(^3P)+M \longrightarrow O_2 + M$	(a) 2.7×10^{-33} (b) $3.0\times10^{-33}\left(\frac{T}{300}\right)^{-2.9\pm0.4}$	6. The temperature-dependence in the new value (b) may have significant effect on mesospheric oxygen chemistry. The winter warming in midlatitude stations will weaker this rate by a factor around.

REACTION	REACTION RATES cm^3/s (2 body); cm^6/s (3 body	REMARKS
7. $O(^3P) + O_3 \longrightarrow 2O_2$	(a) $5.6\times10^{-11}\exp(-5700/RT)$	7. In both (a) and (b) the rate is low, and as can be seen in Fig. 7 and 8, generally smaller than 5 and 6. For ozone loss, this value makes loss through hydrogen (Reaction 14) important in the mesosphere. The value at (c) has been recently quoted in the IAGA Symposium, Toronto (1968).
	(b) $(1.4\pm0.3)\times10^{-12} \cdot e^{-\frac{1500\pm200}{T}}$	
	(c) $1.2\times10^{-11}\exp(-4.0/RT)$	
8. $O(^1D) + O_3 \longrightarrow 2O_2$ M	3×10^{-10}	8. Value recently quoted in the IAGA symposium in Toronto (1968)
9. $O(^1D) + M \longrightarrow O + M$	$1 \times 10^{-10\pm2}$ $(M = O_2)$	
	$5 \times 10^{-11\pm0.5}$ $(M = N_2)$	
10. $O(^1D) + H_2O \longrightarrow 2$ OH	10^{-11}	10. Key reaction for hydrogen products in regions where dissociation of H_2O is negligible. Actual rate may be faster.
11. $O(^1D) + H_2 \longrightarrow$ OH + H	10^{-11}	
12. $O(^3P) +$ OH $\longrightarrow$ H + O_2	10^{-11}	
13. $O(^3P) + HO_2 \longrightarrow$ OH + O_2	1×10^{-11}	13. Actual rate is probably faster. The actual significance of reactions 12 and 13 in the loss of O(3P) depends on OH and HO_2 concentrations. See Fig. 8.

REACTION		REACTION RATES cm^3/s (2 body); cm^6/s(3 body)	REMARKS
14. $O_3 + H \longrightarrow OH + O_2$		2.6×10^{-11}	14. Probably becomes important only above 60 Km. May provide major loss of O_3 in the upper mesosphere.
15. $O_3 + OH \longrightarrow HO_2 + O_2$		5×10^{-13}	
16. $OH + OH \longrightarrow H_2O + O(^3P)$	(a)	2.8×10^{-12}	16. Value at (b) recently quoted in the IAGA symposium in Toronto (1968)
	(b)	2.0×10^{-12}	
17. $O_3 + HO_2 \longrightarrow HO + 2O_2$		10^{-14}	
18. $OH + HO_2 \longrightarrow H_2O + O_2$		10^{-11}	
19. $H + HO_2 \longrightarrow H_2 + O_2$		2×10^{-13}	
20. $H + HO_2 \longrightarrow 2OH$		10^{-11}	
21. $O(^3P) + H_2 \longrightarrow OH + H$	(a)	$4.1 \times 10^{-11} \exp(-7.7/RT)$	21. Value at (b) recently quoted in the IAGA symposium at Toronto (1968)
	(b)	$7 \times 10^{-11} \exp(-10.2/RT)$	
22. $O(^3P) + H_2O_2 \longrightarrow OH + HO_2$		10^{-15}	
23. $O(^3P) + H + M \longrightarrow OH + M$		8×10^{-33}	
24. $O(^3P) + OH + M \longrightarrow HO_2 + M$		1.4×10^{-31}	
25. $O_3 + HO_2 \longrightarrow OH + 2O_2$		10^{-14}	
26. $O_3 + H \longrightarrow HO_2 + O(^3P)$		$2 \times 10^{-10} \exp(-4/RT)$	

REACTION	REACTION RATES Cm^3/s (2 body); cm^6/s (3 body)	REMARKS
27. $HO_2 + HO_2 \longrightarrow H_2O_2 + O_2$	1.5×10^{-12}	27. Quoted in Toronto IAGA symposium (1968)
28. $H + HO_2 \longrightarrow H_2O + (O3P)$	$2 \times 10^{-10} \exp(-4/RT)$	
29. $H + H + M \rightarrow H_2 + M$	2.6×10^{-32}	
30. $H + H_2O_2 \longrightarrow H_2 + HO_2$	10^{-13}	
31. $H + O_2 + M \rightarrow HO_2 + M$	$(5\pm2) \times 10^{-32} \left(\frac{T}{300}\right)^{-2.0\pm0.5}$	
32. $H + O_2 \longrightarrow OH + O(3P)$	$1 \times 10^{-9} \exp(-16.8/RT)$	
33. $H + OH \longrightarrow H_2 + O(3P)$	$1.8 \times 10^{-12} \exp(-5.8/RT)$	
34. $H_2 + OH \longrightarrow H_2O + H$	$10^{-10} \exp(-5.9/RT)$	
35. $H_2O_2 + h\nu \xrightarrow{1875 < \lambda < 3825A} 2OH$		
36. $H_2O + h\nu \xrightarrow{1350 < \lambda < 2375 + L_\alpha} OH + H$	$4.7 \times 10^{-6} \exp(-1.1 \times 10^{-20} \Sigma_{O_2})$	
37. $HO_2 + h\nu \longrightarrow OH + O(3P)$		
38. $O_3 + N \longrightarrow NO + O_2$	$2 \times 10^{-12} T^{1/2} e^{-1200/T}$	

REACTION	REACTION RATES cm^3/s (2 body); cm^6/s (3 body)	REMARKS
39. $N + O_2 \longrightarrow NO + O$	$(1.4 \pm 0.2) \times 10^{-11} e^{-\frac{3600 \pm 200}{T}}$	
40. $N + O_2(^1\Delta_g) \rightarrow NO + O$	$4 \times 10^{-14} < k < 4 \times 10^{-13}$	40. Del Grecо and Kenneally (1968) have found that the rate is in excess of $4 \times 10^{-14} cm^3 sec^{-1}$
41. $N + O \longrightarrow NO + h\nu$	2×10^{-17}	
42. $N + O + M \rightarrow NO + M$	(a) $10^{-32} \left(\frac{T}{300}\right)$	42. Value at (b) quoted at the IAGA symposium in Toronto (1968)
	(b) 9×10^{-33}	
43. $N + NO \longrightarrow N_2 + O$	2.2×10^{-11}	
44. $NO^+ + e \longrightarrow N + O$	$5 \times 10^{-7} \left(\frac{300}{T}\right)$	44. This reaction possibly provides the major source of atomic nitrogen in the lower thermosphere.
45. $N_2^+ + O \longrightarrow NO^+ + N$	$(2.5 \pm 0.8) \times 10^{-10}$	
46. $e + O_3 \longrightarrow O^- + O_2$	$(1\text{-}10) \times 10^{-12}$	
47. $O_3^- + h\nu \longrightarrow O_3 + e$	$\sim 10^{-2}$	
48. $O_2^- + O_3 \longrightarrow O_3^- + O_2$	3.0×10^{-10}	48. Major reaction through which ozone controls [illegible]

REACTION	REACTION RATES cm^3/s (2 body); cm^6/s (3 body)	REMARKS
49. $O^- + O_3 \rightarrow O_3^- + O$	7.0×10^{-10}	
50. $O_3^- + CO_2 \rightarrow CO_3^- + O_2$	4×10^{-11}	
51. $O_3^- + NO \rightarrow NO_3^- + O$	1×10^{-11}	
52. $CO_3^- + O \rightarrow O_2^- + CO_2$	8×10^{-11}	
53. $NO_2^- + O_3 \rightarrow NO_3^- + O_2$	2×10^{-11}	
54. $O_2^- + O \rightarrow O_3 + e$	2.5×10^{-10}	54. Provides the main detachment process for O_2^- ion, the primary negative ion. Any variation of O can have provound influence on negative ion balance.

is not so apparent in the oxygen-hydrogen calculations of Hunt or Hesstvedt.

The latitudinal contours given by London (1968) are for the region 15 - 60 Km. London also considered the possible seasonal variation arising from the changes in atmospheric temperature as well as, of course, the changes in mean solar zenith angle. Changes in the characteristic time for ozone from summer to winter given in Fig.2 are of interest. There is little latitudinal variation in summer, but large variation in winter. In summer it decreases from about 3 years at 20 Km to less than one hour at 55 Km. At polar latitudes in winter large characteristic times are found upto about 35 Km. Above 45 Km these times are, however, reduced to less than one day at all latitudes. The large winter characteristic times at high latitudes allows polar accumulation of ozone transported from equatorial regions, resulting in an increase in ozones.

3. Oxygen-Hydrogen Atmosphere

The need for including hydrogen reaction in the O-O_3 scheme was first recognized by Bates and Nicolet (1950) who emphasised the significance of the identification of the Meinel bands of the airglow with OH. Indeed the hydroxyl emission may very well hold the clue to the $O - O_3$ problem. The dawn decay of the hydroxyl emission occurs through the hydrogen-ozone reaction :

$$H + O_3 \longrightarrow OH + O_2$$

which has a rate coefficient of $2.6 \times 10^{-11} cm^3/s$ and can be an important participant in ozone photochemistry if hydrogen concentration is large. Direct photodissociation of H_2O at heights above 60 Km, and at lower heights the indirect process :

$$O(^1D) + H_2O \longrightarrow 2OH$$

followed by

$$OH + O \longrightarrow O_2 + H$$

$$H + O_2 + M \longrightarrow HO_2 + M$$

$$HO_2 + HO_2 \longrightarrow H_2O_2 + O_2$$

provide the source for the various hydrogen products.

The different reactions involved in the oxygen-hydrogen system and their rate coefficients are summarised in Table 2. Where more recent values are available, they are indicated under (b). The rates are in many cases quite uncertain, and in some cases very strongly dependent on temperature. Variations of the reaction rates with latitude and season, of the dissociation rates (J's) with solar zenith angle, and of atmospheric density should be taken into account if the computations are to be complete. This, however, is not feasible when so many reactions are involved.

Not all reactions are, however, important. Considerable simplification is possible through the examination of Figs.7 and 8 in which the production and loss process for O and O_3 are plotted for an ozone distribution suggested by Evans et al (1968) combining the Johnson et al observations

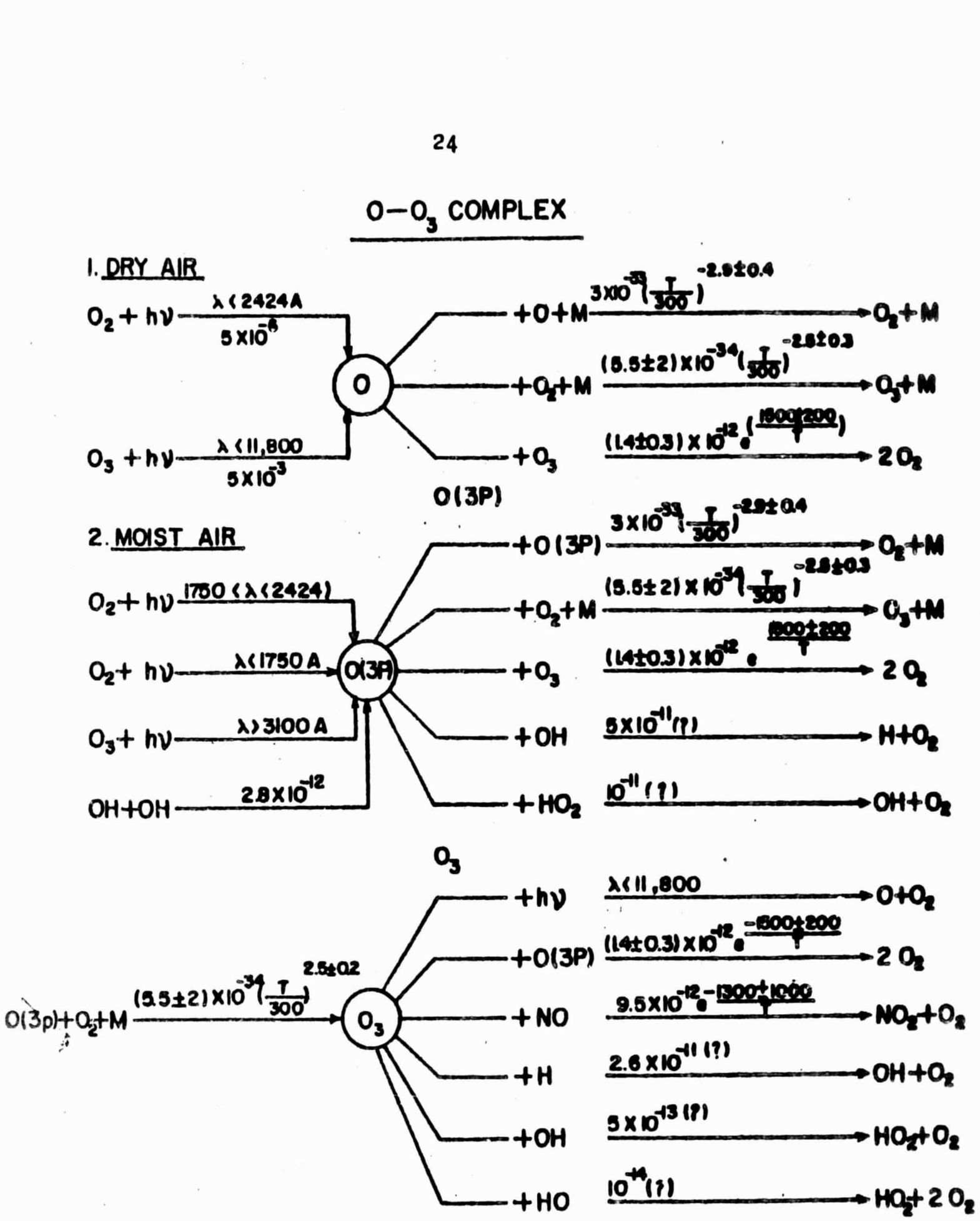

Fig.6 Schematic diagram giving important reactions in the production and loss of atomic oxygen and ozone with current values of reaction rates.

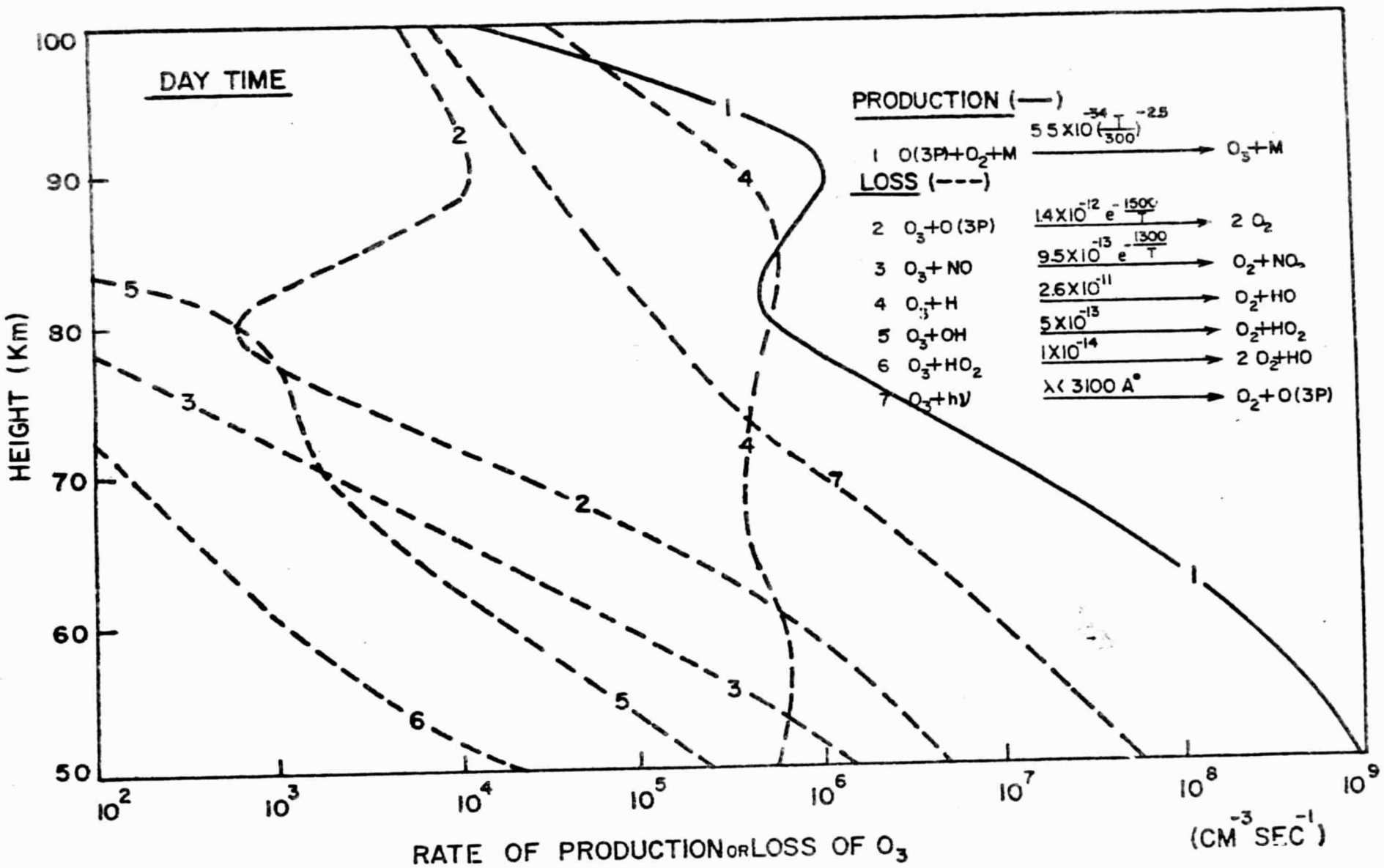

Fig.7.a Height distribution of atomic oxygen production and loss rates for each reaction. Note that not all reactions are important. From these curves it is possible to select the dominant reactions for each height. Curves (a) are for daytime and curves

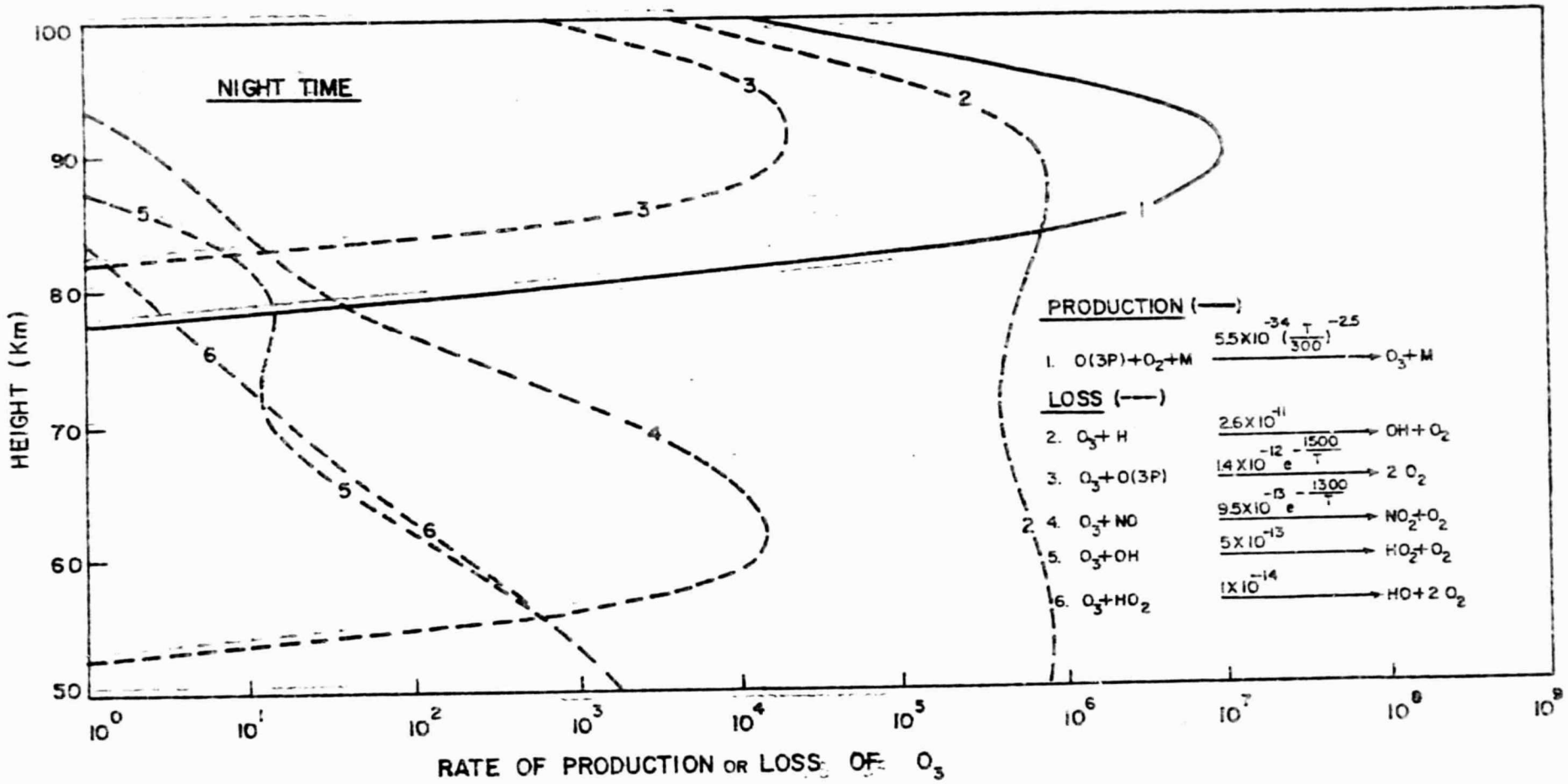

Fig.7. b Height distribution of atomic oxygen production and loss rates for each reaction. Note that not all reactions are important. From these curves it is possible to select the dominant reactions for each height. Curves (b) for night.

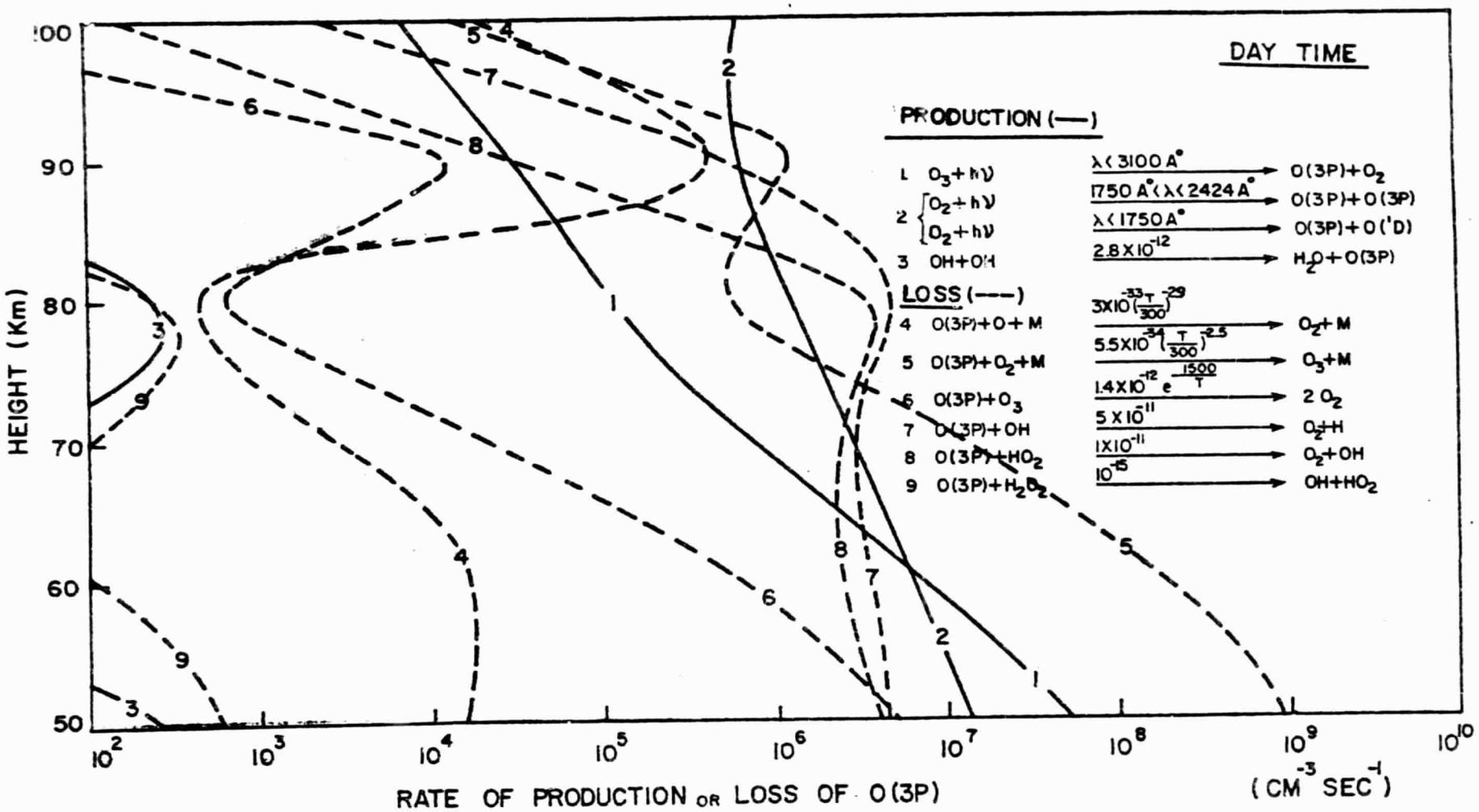

Fig.8.a, Height distributions of ozone production and loss rates for each reaction. Note that not all reactions are important. From these curves it is possible to select the dominant reactions for each height. Curves (a) are for daytime and curves

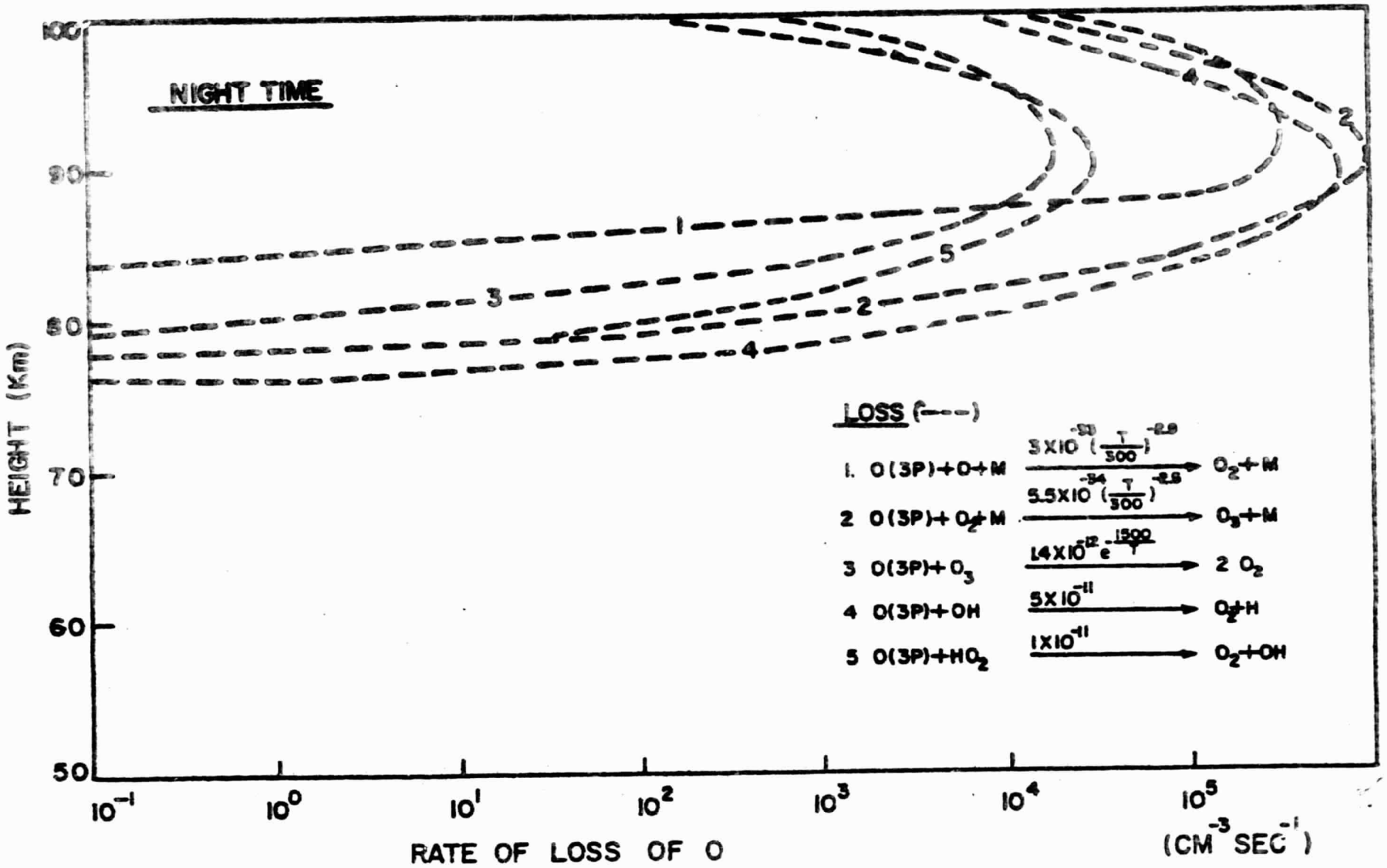

Fig.8. ,b Height distributions of ozone production and loss rates for each reaction. Note that not all reactions are important. From these curves it is possible to select the dominant reactions for each height. Curves (b) for night.

below 70 Km with those estimated from observations of metastable O_2 (Evans et al, 1968). For atomic oxygen no experimental values are available, and theoretical models must be used. We have used the models given by Hesstvedt. For the present purpose, i.e. identification of the principal processes, the exact O-model used is not critical. For other minor constituents, Hesstvedt's models are used, excepting for NO for which Pearce's (1969) new recent rocket results are used.

In the light of these calculations, the number of important processes can be brought down to an usuable number even for the oxygen-hydrogen case. Schematic diagrams for dry air and moist air cases subjected to such selection enteria are given in Fig.6.

The neutrals we are concerned with are : $O(^3P)$, $O(^1D)$, O_3, OH, HO_2, H_2O, H_2O_2, H_2 and H. For each level the total amounts of oxygen and hydrogen can be assumed to be constant, as follows (Hesstvedt, 1968).

$$\left[n(O^1D)+n(O^3P)+n(OH)+n(H_2O)\right]/2+n(O_2)+n(HO_2)+n(H_2O_2) + 3n(O_3)/2 = \alpha M \qquad (\alpha = 0.2095)$$

$$\left[n(OH)+n(HO_2)+n(H)\right]/2+n(H_2O_2)+n(H_2)+n(H_2O) + \beta M \qquad (\beta = 8 \times 10^{-6})$$

which, for all practical purposes, can be written simply as :

$$n(O_2) + n(O)/2 = \alpha M$$

$$n(H)/2 + n(H_2) + n(H_2O) = \beta M$$

Hesstvedt identifies three separate regions :

(i) 100-115 Km (ii) 70-100 Km (iii) 45-70 Km. A fourth region bK45 Km has also to be considered. The principal characteristics of these four regions are as follows :

Region I . h ~ 100 - 115 Km

Constituent	Characteristic time	Photochemical status.
O_3	10^2 sec	P.E.*
O	$>10^5$ sec	
OH, HO_2	< 1 sec	P.E.
H_2O_2	$\frac{1}{2}$ - 3 hrs	P.E.
H_2, H_2O	large	

$$n(O_3) = \frac{5.5 \times 10^{-23}(300/T)^{2.5} n(O)n(O_2)n(M)}{5 \times 10^{8}+0.14\exp(-1500/T)\ n(O)+2.6\ n(H)}$$

Region II : h ~ 45 - 70 Km

All, except H_2 and H_2O have small characteristic times. Dominating terms are $J_3 n(O_3)$ and $k_2\ n(M)\ n(O)n(O_2)$. $\tau(O_3)$ is large at night and consequently there is no diurnal variation. For atomic oxygen, the characteristic time at night is about 1/2 hour, and the photochemical equilibrium value for atomic oxygen is given by :

$$\left| n(O_n) \right|_{P.E} = 5 \times 10^{21} \left(\frac{T}{300}\right)^{2.5} \frac{n^2(OH_n)}{n(M)n(O_2)}$$

The day time value for atomic oxygen for heights below 88 Km, where the characteristic time is shorter for atomic oxygen than for ozone, is given by :

$$n(O)_d = \frac{10^{11}\left[J_3 n(O_3) + 2J_2 n(O_2)\right]}{5.5 \times 10^{-23}\left(\frac{T}{300}\right)^{-2.5} n(M)n(O_2)+5n(OH)_d+n(HO_2)_d}$$

---

* P.E. Stands for Photochemical Equilibrium.

Region III : 70 - 100 Km.

The characteristic time for O is increasing very rapidly in this height range, and a marked change occurs at 80 Km, where τ (O) is of the order of a day. O_3, OH, HO_2 and H_2O_2 have short life-times, and their daytime concentrations are given by

$$n(O_3)_d = \frac{5.5 \times 10^{-34}\left(\frac{T}{300}\right)^{2.5} n(M)n(O_2)n(O_d)}{10^{11}J_3 + 2.6\, n(H_d)}$$

$$n(HO_2)_d = \frac{7.4 \times 10^{-21} n(M)n(O_2)n(H_d)}{n(O_d)}$$

$$n(OH,_d) = \frac{n(HO_2)_d n(O_d) + 2.6n(H_d)\, n(O_{3,d})}{5n(O_d)}$$

$$n(H_2O_2,_d) = \frac{30n^2(HO_{2,d})}{10^{-9}H_2O_2 + 10^{-2}n(O_d) + 4n(OH_d) + n(H_d)}$$

For H_2O and H_2 the characteristic times are large. For water vapour it is 3 days at 100 Km and more than 1 month below 75 Km. For H_2, the time is about one month throughout this region.

4. OXYGEN-HYDROGEN ATMOSPHERE WITH EDDY DIFFUSION

Both vertical mean motion and vertical eddy diffusion can be important. Two major works exist dealing with the effect of eddy diffusion in the O-O_3 complex. These come from Hesstvedt (1968) Shimazaki (1967) and Shimazaki and Laird (private communication).

The continuity equation for the i^{th} constituent can be written as

$$\frac{\partial n_i}{\partial t} = Q_i(n_j) - L_i(n_i, n_j) - \frac{\partial \Phi_i}{\partial z}$$

where $j \neq z$, and the three terms on the righthand side are the production, the loss, and the transport terms. In this it is assumed that horizontal mean motion and horisontal eddy diffusion are of less importance than vertical mean motion and vertical eddy diffusion. The average of total vertical flux in a unit time is given by :

$$\Phi = \overline{n_i \omega_i} = \overline{n_i} \overline{u_i} + \overline{n'_i u'_i} = \phi_i + \Psi_i$$

where ϕ_i represents the flux due to the mean motion, and can be evaluated from :

$$\frac{\partial u_i}{\partial t} = - \frac{kT}{m_i} \left(\frac{u_i}{D_{13}} + \frac{1}{n_i} \frac{\partial n_i}{\partial z} + \frac{1}{T} \frac{\partial T}{\partial z} + \frac{1}{H_i} \right)$$

and Ψ_i represents the flux due to the turbulent mixing motion, and can be described in terms of the vertical eddy diffusion coefficient D_{eddy} by (Colegrove, Hanson and Johnson, 1965) :

$$\Psi_i = \overline{n'_i u'_i} = - D_{eddy} \Sigma \bar{n}_i \frac{\partial (\bar{n}_i / \Sigma \bar{n}_i)}{\partial z}$$

$$= - D_{eddy} \left(\frac{\partial \bar{n}_i}{\partial z} - \frac{\bar{n}_i}{\Sigma \bar{n}_i} \cdot \frac{\partial \Sigma \bar{n}_i}{\partial z} \right)$$

The value of the vertical eddy diffusion coefficient and its variation with height is not well known. Hesstvedt (1968) used values varying from $4 \times 10^5 cm^2/s$ at 65 Km te

$7 \times 10^6 cm^2/s$ at 100 Km. Shimazaki (private communication) has tried a number of D_{eddy} models. These include constant values of 10^6 and $10^7 cm^2 sec^{-1}$ and a model in which the coefficient varies linearly from $5 \times 10^5 cm^2 sec^{-1}$ at 40 Km to $5 \times 10^6 cm^2 sec^{-1}$ at 100 Km and remaining constant (at $5 \times 10^6 cm^2/sec$) above 100 Km.

Hesstvedt's 'eddy diffusion model' extends from 65 to 100 Km; at these two boundaries photochemical values were taken. The assumption of photochemical equilibrium is quite justified at 65 Km; but that at 100 Km is questionable, and it would seem more realistic to start from a level (such as 120 Km) where measurements of the ratio O/O_2 exist. Calculation by Shimazaki and Laird (private communication) extend from 40 to 150 Km.

The inclusion of eddy diffusion in the calculation brings in some very major changes above 80 Km, specially in the hydrogen components H, H_2 and H_2O. The concentration of water vapour which has a long characteristic time is considerably increased, taking up 85 % of all available hydrogen at 80 Km. The distributions of water vapour, with and without eddy diffusion, are shown. There are also increases in OH and HO_2 which appear to have a serious consequence in O-distribution, since these increased concentration now provide a very effective sink for atomic oxygen through the reactions :

$$OH + O(3P) \longrightarrow H + O_2$$

$$HO_2 + O(3P) \longrightarrow OH + O_2$$

In consequence, there is a pocket of low atomic oxygen in Hesstvedt's model near 80 Km. The other major effect on atomic oxygen is the appearance of a broad maximum centred around 90 - 95 Km in place of a pronounced peak at 100 Km obtained under the condition of photochemical equilibrium.

5. OXYGEN - HYDROGEN - NITROGEN ATMOSPHERE

A further complication, normally ignored, is that there are also a number of reactions involving O and O_3 with a number of nitrogen compounds, especially nitric oxide. The important nitrogen-oxygen reactions are also summarised in Table 2 alongwith current values of their reaction rates. Since most nitrogen compounds have low concentrations, they do not seriously affect the concentration of O or O_3, so that in describing the variations of O and O_3, it is generally immaterial whether or not we consider the nitrogen reactions. There are, however, two reasons why these should not be ignored. One is that the concentrations of nitrogen compounds such as NO, NO_2 and N_2O are very critically dependent on the concentrations of O and O_3, so that any observations on latter may ultimately lead to an information on the former. The other is that one of these nitrogen compounds, namely NO, is also easily ionized and in fact contributes a large part of the D region ionization. This ionization is being measured with increasing reliability by a wide variety of groundbased and rocketborne techniques, and can, in principle, provide information of considerable value to ozone photochemistry.

The principal reactions concern NO, Nitric oxide appears to be quite abundant in the mesosphere, although there is considerable dispute about how abundant it actually is. Rocket measurements reported by Barth (1966) and very recently by Pearce (1969) place its concentration at 70 Km between 10^8 - $10^9 cm^{-3}$ and at 90 Km between 10^7 and $10^8 cm^{-3}$. Ionospheric estimates are one to two orders of magnitude lower.

It seems fairly certain that O_3 provides a powerful sink for NO below 70 Km through the reaction :

$$NO + O_3 \rightarrow NO_2 + O_2$$

which has a rate constant of $9.5 \times 10^{-13} cm^3/s$.

That this, in fact, does occur is observed in the results given by Pearce in which a sudden change in slope is observed below 70 Km. Thus at this level nitric oxide, ozone reaction begins to take over from the usual nitric oxide, atomic nitrogen reaction :

$$N + NO \rightarrow N_2 + O$$

The reactions participating in the production and loss of NO including those involving O and O_3 are given in Table 3. If at 70 Km, the two loss rates are assumed to be equal, then, using the rates given in Table 2.

$$n(O_3) = 9 \times 10^3 n(N)$$

The observational results of ozone vary from 3×10^8 to $1 \times 10^9 cm^{-3}$ at 70 Km, giving

TABLE 3

PRINCIPAL REACTIONS FOR NITRIC OXIDE IN THE MESOSPHERE AND LOWER THERMOSPHERE

MAJOR REACTIONS

1.	$N + O_2 \xrightarrow{b_7} NO + O$	$b_7=(1.4\pm0.2)\times10^{-11}e^{-\frac{3600\pm200}{T}}$ cm^3/s
2.	$N + O+M \xrightarrow{b_{1a}} NO+M$	$b_{1a}=1.1\times10^{-32}\frac{T}{300}$ cm^6/s
3.	$N + \blacksquare \xrightarrow{b_{1b}} NO+h$	$b_{1b}=2.10^{-17} cm^3/s$
4.	$N + NO \xrightarrow{b_6} N_2+O$	$b_6=2.2\times10^{-11} cm^3/s$
5.	$N+O_2(^1\Delta_g) \xrightarrow{k} NO+O$	At least $4 \times 10^{-14} cm^3/s$, may be 10 times or more larger.

ADDITIONAL PROCESSES LIKELY TO BE IMPORTANT

6.	$O_2^+ + N_2 \xrightarrow{\gamma_7} NO^+ + NO$	$\gamma_7=1\times10^{-17\pm2} cm^3/s$
7.	$NO+O_3 \xrightarrow{b_4} NO_2+O_2$	$b_4=9.5\times10^{-13}e^{-\frac{1300\pm100}{T}}$ cm^3/s
8.	$O_2^+ + NO \xrightarrow{\gamma_5} NO^+ + O_2$	$\gamma_5=(8\pm2)\times10^{-10} cm^3/s$
9.	$NO_2+h\nu \xrightarrow{J_{NO}} NO+O$	$J_{NO} \simeq 5\times10^{-3}$
10.	$O + NO_2 \rightarrow NO+O_2+46$ Kcal	$(2.8\pm0.9)\times10^{-11}e^{\frac{-550\pm100}{T}}$

ERRATA FOR RPU SCIENTIFIC REPORT NO.47

Page	Line	Should read as
7	Equation 1	$\frac{dn(o)}{dt} = 2J_2n(O_2) + J_3n(O_3) - 2K_{11}n^2(O)n(M) - K_{12}n(O)n(O_2)n(M) - K_{13}n(O)n(O_3)$
7	Equation 2	$\frac{dn(O_3)}{dt} = K_{12}n(O)n(O_2)n(M) - J_3n(O_3) - K_{13}n(O)n(O_3)$
7	Equation 3	$\frac{n(O_3)}{n(O)} = \frac{K_{12}n(O_2)n(M)}{J_3 + K_{13}n(O)}$
15	Equation 1st Table 2, Column 3.	$J = \int_{\lambda_1}^{\lambda_2} A_\lambda Q_{\alpha\lambda} e^{-\tau_\lambda} d\lambda$
30	2nd Equation	$\left[n(O)_n\right]_{P.E} = 5\times10^{-21} \left(\frac{T}{300}\right)^{2.5} \frac{n^2(H)_n}{n(M)n(O_2)}$
31	1st Equation	$n(O_3)_d = \frac{5.5\times10^{-34} \left(\frac{T}{300}\right)^{2.5} n(M)n(O2)n(O)_d}{10^{11}J_3 + 2.6n(H)_d}$
31	2nd Equation	$n(HO_2)_d = \frac{7.4 \times 10^{-21}n(M)n(O_2)n(H)_d}{n(O)_d}$
31	3rd Equation	$n(OH)_d = \frac{n(HO_2)_dn(O)_d + 2.5n(H)_dn(O_3)_d}{5n(O)_d}$
31	4th Equation	$n(H_2O_2)_d = \frac{30n^2(HO_2)_d}{10^{-9}n(H_2O_2) + 10^{-2}n(O)_d + 4n(OH)_d + n(H)_d}$
32	2nd Equation	$\Phi_i = \overline{n_iw_i} = \overline{n\mu_i} + \overline{m'_iu'_i} = \varphi_i + \psi_i$
32	3rd Equation	$\frac{\partial u_i}{\partial t} = \frac{-KT}{m_i}\left(\frac{u_i}{D_{i3}} + \frac{1}{n_i}\frac{\partial n_j}{\partial x} + \frac{1}{T}\frac{\partial T}{\partial x} + \frac{1}{H_i}\right)$
44	2nd Equation	$q = \frac{\beta_\alpha n^2(O_2)}{1 + \frac{\rho + K_an(O)}{K_e n(O_3)}} N_e + \alpha_D n(xy^+) N_e$

$$n(N) \sim (3 - 10) \times 10^4 cm^{-3}$$

Any variation in either constituent will affect the transition level.

Although at levels below 70 Km, the nitric oxide, ozone reaction provides the major source for the loss of nitric oxide, it does not affect O_3 concentration. At 70 Km, the ozone loss rate per ozone molecule for the different reactions given in Fig.9 are :

O, O_3 reaction	10^{-5} $cm^{-3}sec^{-1}$
H, O_3 reaction	$2.6 \times 10^{-4} cm^{-3}sec^{-1}$
OH, O_3 reaction	$1.5 \times 10^{-8} cm^{-3}sec^{-1}$
HO_2, O_3 reaction	$1.5 \times 10^{-8} cm^{-3}sec^{-1}$
NO, O_3 reaction	$2.3 \times 10^{-6} cm^{-3}sec^{-1}$ (Pearce model)
O_3 dissociation	10^{-5} cm^{-3} sec^{-1}

Thus at this height the principal loss is through Hydrogen-ozone, oxygen-ozone and photodissociation of ozone and although nitric oxide, ozone loss rate is larger than those of (OH, O_3) and HO_2, O_3) reactions, it is still unimportant.

There may, however, be a drastic change after sunset. Atomic hydrogen concentration at heights below 80 Km is now negligible. In contrast the twilight observations of NO and photochemical considerations for nighttime situation show that the NO concentration is large at least down to 70 Km. Thus at night nitric oxide may provide an important loss process for ozone and may well be responsible for the low pocket of O_3 sometimes observed in nighttime records.

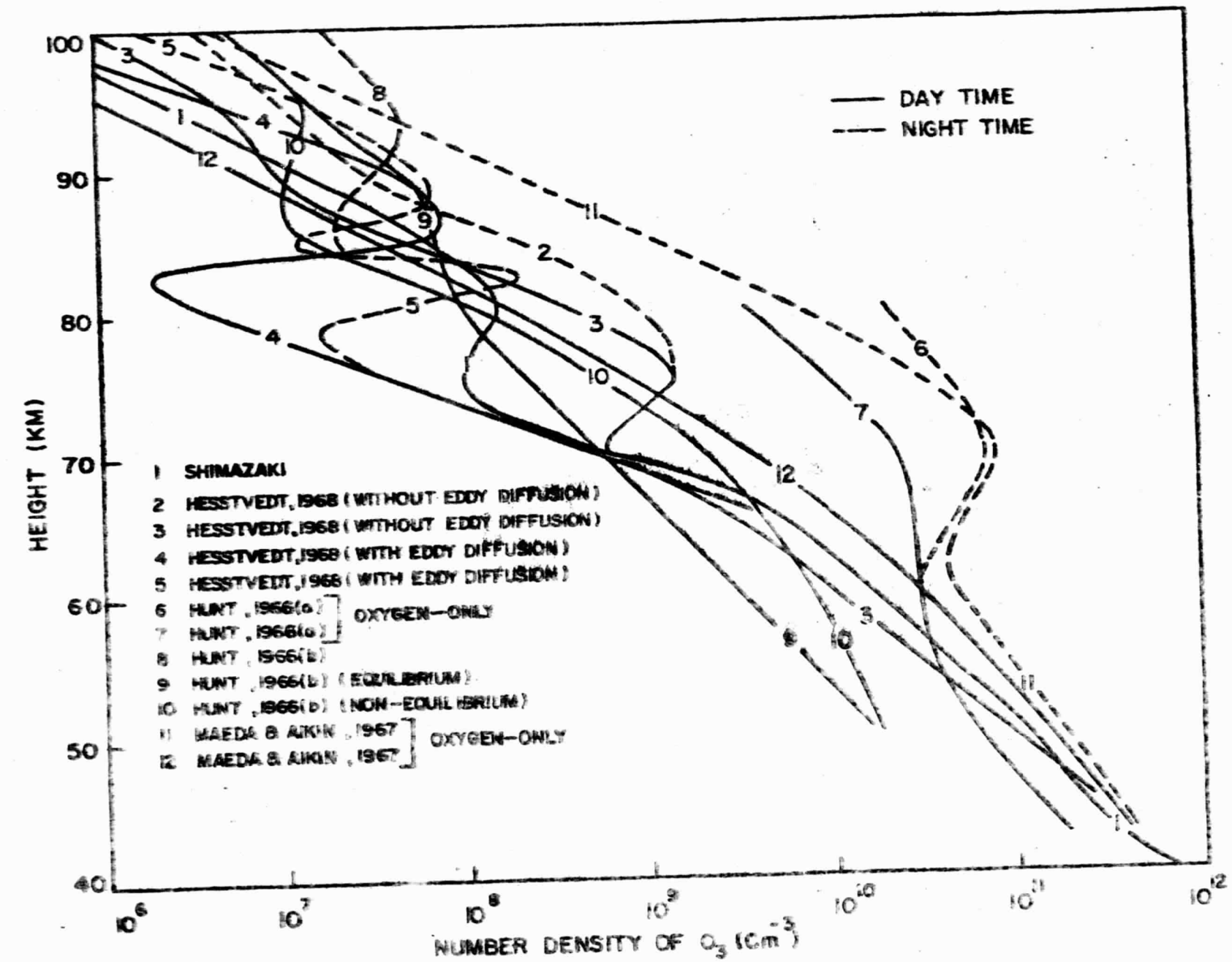

Fig.9 Photochemical distributions of ozone obtained by different workers under different assumptions. Note the differences in the distributions. The distribution given by Shimazaki and Laird (private communication) is for an oxygen-hydrogen-nitrogen atmosphere.

6. OZONE VARIATIONS DURING A SOLAR ECLIPSE

Photochemical calculations of the variations of ozone concentration in the mesosphere were carried out by Hunt (1965) for an eclipse in which the time from first contact to fourth contact is 9000 seconds and no solar radiation reaches the earth at the time of totality at 4500 seconds. Computations have also been made for two specific cases : for the eclipse of July 1963 by Doherty (private communication) and the eclipse of November 12, 1966 by Keneshea (1966). Keneshea's computations consider not only the neutral atmospheric species, but also the positive and negative ions, and are thus more complete. Some of these calculations, alongwith rocket measurement of Randhawa for the November eclipse, are shown in Fig.10. Keneshea's computations give an order of magnitude increase in O_3 concentration between 60 - 100 Km as photo-dissociation of O_3 is gradually cut off and an increasing amount of ozone is being formed through the three body reaction :

$$O + O_2 + M \rightarrow O_3 + M$$

which has a reaction time of about 10^3 seconds at 70. Since these times are small in comparison with the time of the eclipse, one expects that a change in O_3 will occur. Maximum enhancement occurs about 10 minutes after totality. Randhawa's (1968) observations with rocketborne ozonesonde during the eclipse of November 12, 1966 at Tartagal ($22^{o}32'S$, $63^{o}50'W$), Argentina showed that ozone concentration at 57 Km during total solar eclipse was about 2.5 times higher than that measured a

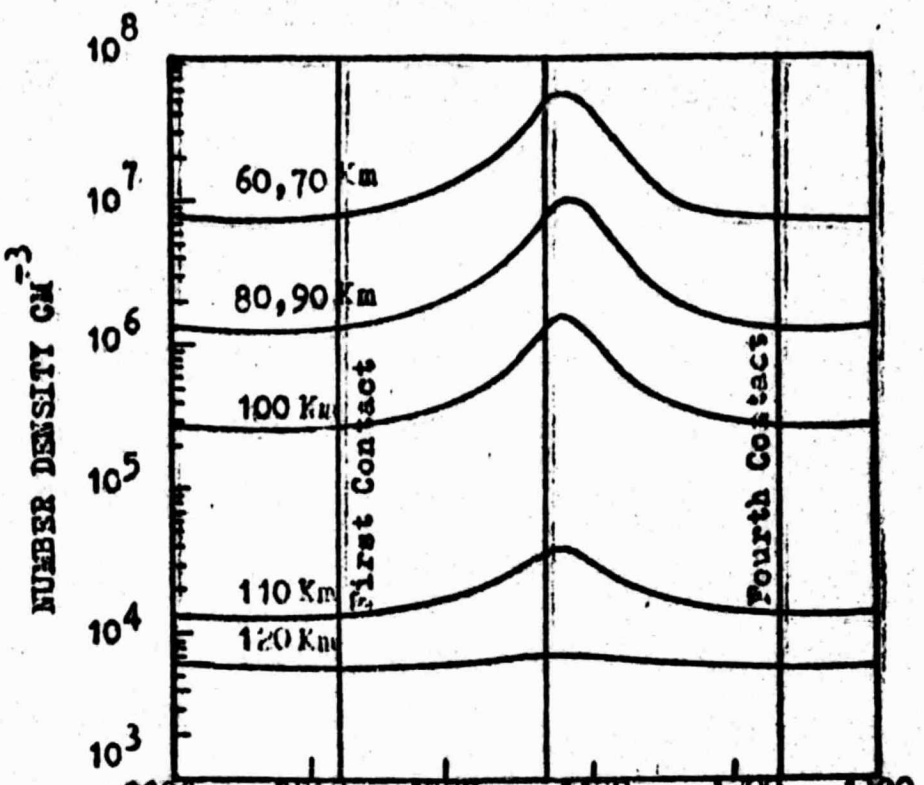

Fig.10 Keneshea's computations on changes in ozone concentrations during the solar eclipse of November 12, 1966.

day earlier at the same altitude. The increase in ozone during total solar eclipse was found to be rapid.

7. OZONE AND MESOSPHERIC IONIZATION

Doherty (1968) has identified a curious resemblance between the computed variation in ozone concentration and mesospheric ionization during the July 1963 solar eclipse (Fig.11). The suggested explanation is that an increase in ozone can deplete N_e through the chain indicated in Fig.12. In the negative ion scheme outlined in Fig.12, most of the electrons that attach to 02 to form 02^- immediately (time constant at 70 Km is 0.6 sec) return to their original state through the reaction :

$$O_2^- + O \longrightarrow O_3 + e$$

which has a very fast rate of $10^{-10} cm^3/s$. A smaller part of the O_2^- ions will charge transfer with O_3 molecules to form O_3^- ion (5 sec.)

$$O_2^- + O_3 \longrightarrow O_3^- + O_2 \quad (4x10^{-10} cm^3/s)$$

Although these constitute only the beginning of the chain, the vital role played by O_3 and O are derived. It is clear that a decrease in electron density occurs by : (a) an <u>increase</u> in ozone concentration and also by (b) a decrease in atomic oxygen concentration. Both conditions are satisfied during an eclipse.

Similar situation exists during the sunset period; when with night fall there is an increase in O_3 and a decrease in

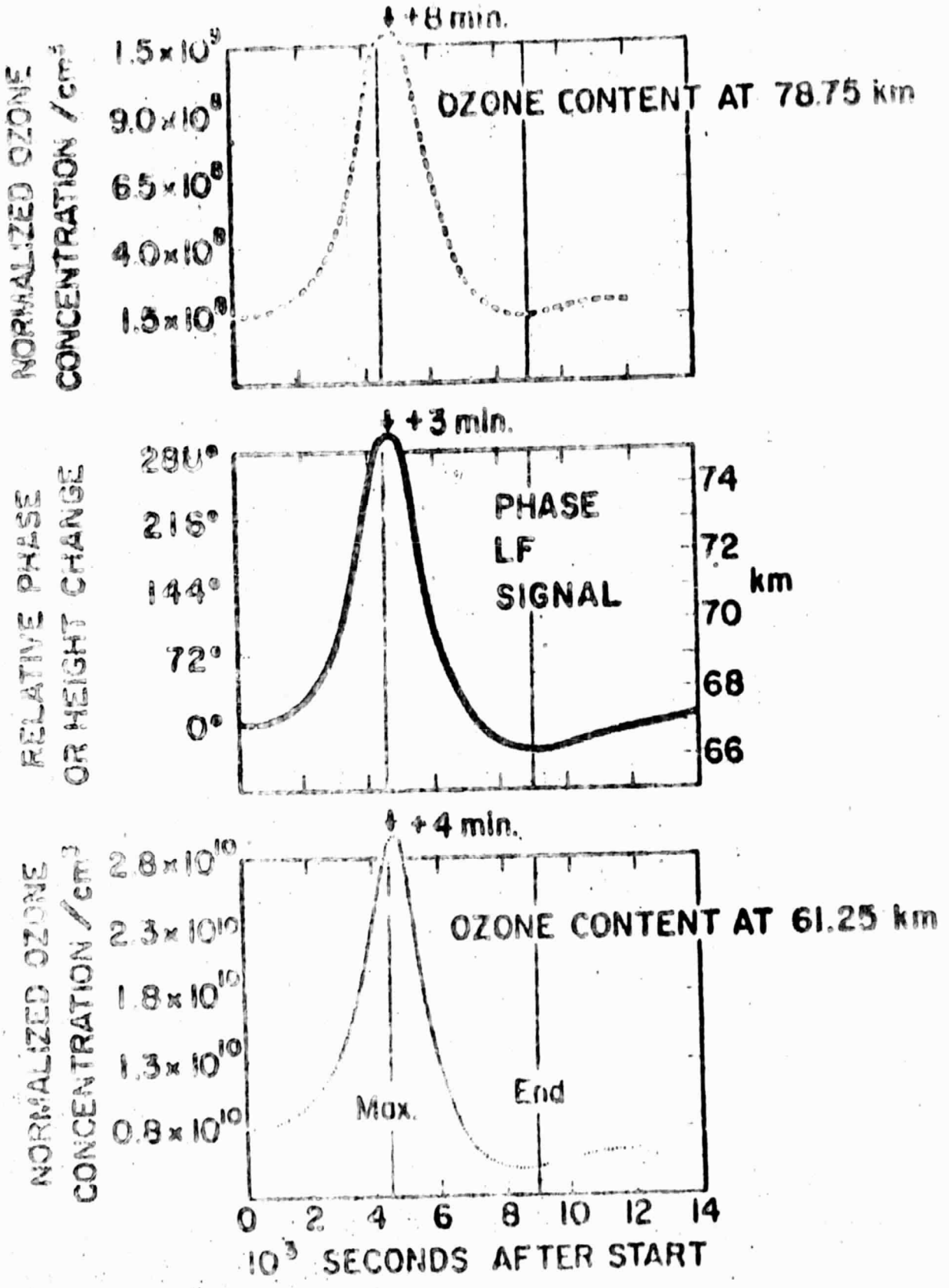

Fig.11 Variations in LF phase compared with changes in ozone concentrations during the solar eclipse of July 1963.

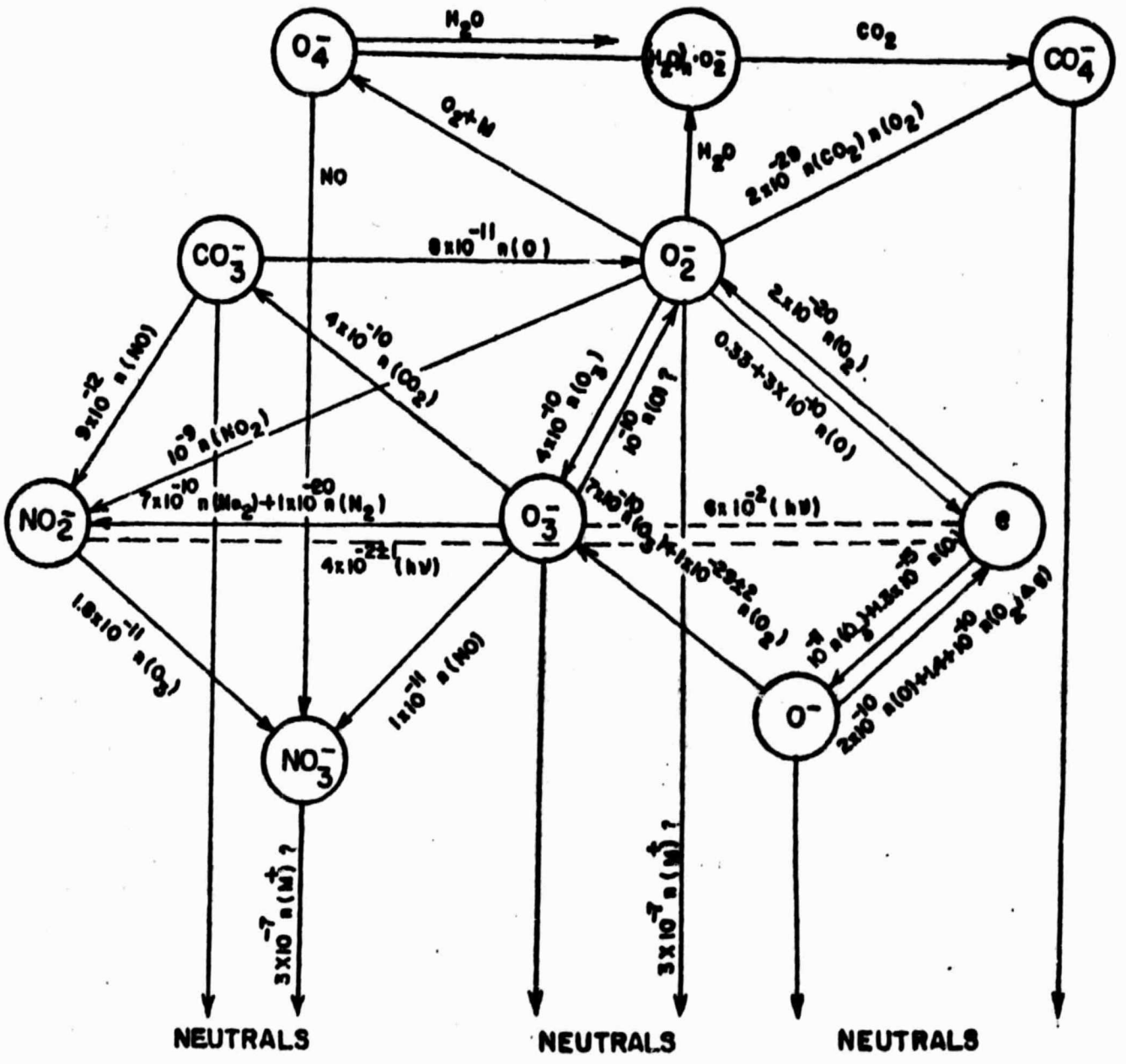

NEGATIVE ION SCHEME

Fig.12 Negative ion scheme with current reaction rates.

atomic oxygen.

If this explanation is correct, then variations in atomic oxygen or ozone in the mesosphere should be observed through changes in mesospheric ionization. In simple terms, the two are than related through the equation :

$$\gamma(O,O_3) = q/N_e^2$$

where $\gamma(O, O_3)$ is the effective loss rate, q the rate of electron prediction and N_e, the electron density.

The exact relationship relating $\gamma(O, O_3)$ with the concentration of O and O_3 depends, of course, on the exact nature of the negative ion scheme assumed. Bowhill and Radicella (1968), considering only the reactions :-

$$O_2 + O_2 + M \longrightarrow O_2^- + O_2 \qquad (\beta a)$$

$$O_2^- + h\nu \longrightarrow O_2 + e \qquad (\rho)$$

$$O_2^- + O \longrightarrow O_3 + e \qquad (ka)$$

$$O_2^- + O_3 \longrightarrow O_3^- + O_2 \qquad (k\alpha)$$

$$XY^+ + e \longrightarrow X + Y \qquad (\alpha_D)$$

derived the following expression :-

$$q = \frac{\beta a\, n(O_2)^2}{1 + \dfrac{\rho + k_a n(O)}{k_\alpha n(O_3)}} N_e + \alpha_D\, n(XY^+) N_e$$

from the observed variation of N_e during the solar eclipse of November, 1966, he and his colleagues concluded that the ozone concentration increased by as much as 100 times at 75 Km during totality.

The calculations of Bowhill et al were examplified, since the channel $e \xrightarrow{2O_2} O_2^- \xrightarrow{O_3} O_3^-$ does not terminate

at O_3^- and the subsequent fate of O_3^- down the line to NO_3^- (or a similar long enduring ion) or via CO_3^- to O_2^- to electrons must be known. There are several reasons why the exact involvement of O or O_3 in negative ion variation cannot at present be quantitatively discussed; one major reason being the obsence of any process that could normally lead the negative ions away from O_2^-. An interesting consequence of the present negative ion theory is that :

$$\frac{\lambda(CO_3^-)}{\lambda(O_2^-)} \simeq 5 \frac{n(O_3)}{n(O)}$$

and that NO_2^- and NO_3^- ions which are subsequently formed from CO_3^- ions are given by : $\lambda(NO_2^-) = \dfrac{0.1\, n(NO)\, \lambda(CO_3^-)+10n(NO_2)\, \lambda(O_2^-)+7n(NO_2)\, \lambda(O_3^-)}{0.2\, n(O_3)+3x10^3 n^+ +4x10^8}$

$$\lambda(NO_3^-) = 6 \times 10^{-5} n(O_3) \frac{\lambda(NO_2^-)}{n^+} + 3 \times 10^{-5} n(NO) \frac{\lambda(O_3^-)}{n^+}$$

With current laboratory rates O_2^- associate detachment process is the controlling factor, and the negative ions in the daytime mesosphere, almost exclusively O_2^-, are given by :

$$\lambda(O_2^-) = 7 \times 10^{-21} \frac{n^2(O_2)}{n(O)}$$

Observational estimates, including those recently obtained through rocket borne soundings, indicate that λ is between 1 to 10 at 70 Km during daytime. If these results are accepted and current laboratory rates are believed, then atomic oxygen concentration must be low at these heights; and with $\lambda = 1$ at 70 Km, n(O) cannot be much in excess of $7 \times 10^8 cm^{-3}$. This is a very low value, and quite inconsistent with the photochemical model of Hunt (which gives a value of about $5 \times 10^{10} cm^{-3}$ at 70 Km). Hesstvedt's 'Eddy diffusion model', comes closest to this requirement : his 'low' atomic oxygen concentration, under the conditions of eddy diffusion, is about $6 \times 10^9 cm^{-3}$ at 70 Km and $1.4 \times 10^9 cm^{-3}$ at 80 Km.

The requirements of mesospheric ionization and in particular of negative ions are not normally considered in photochemical theories of ozone. This is a serious omission.

References

Aikin C.A. and Kai-kai Maeda	1967	Temporal variations of mesospheric oxygen and ozone during auroral events; NASA TN D-3993, Nov.1967
Barth C.A.	1968	Nitric oxide in the Upper atmosphere, Ann. Geophys., 24, 198, 1968.
Benson, S.W. and Axworthy A.E.	1965	Reconsiderations of the rate constants from the thermal decomposition of ozone, J. Chem. Phys., 42, 2614-2615,
Bowhill S.A. and Radicella S.M.	1968	U.S. URSI meeting, Washington.
Carver, J.H., Horton, B.H. and Burger, F.G.	1968	Nocturnal ozone distribution in the upper atmosphere, J.G.R., 71, 4189.
Chapman S	1930	On ozone and atomic oxygen in the upper atmosphere, Phil. Mag. 10, 369.
Colegrove, F.D., Hanson W.B. and Johnson, F.S.	1965	Eddy diffusion and oxygen transport in the lower thermosphere, JGR, 70, 4931.
Doherty, L.H.	1968	Importance of associative detachment and dissociative attachment in lower ionosphere as shown by LF radio measurements, JGR, 73 (No.7), 2429.
Hesstvedt,E	1963	On the determination of characteristic times in a pure oxygen atmosphere, Tellus, 82-88.
Hesstvedt, E	1965	The ozone distribution over the equator and its dependence on vertical motions, Tellus, 17, 177,
Hunt B.G.	1965	A theoretical study of the changes occurring in the ozonosphere during a total solar eclipse of the sun, Tellus, 17,516.
Hunt, B.G.	1965	A nonequilibrium investigation into the diurnal photochemical atomic oxygen and ozone variation in the mesosphere, J.A.T.P., 27, 133.
Hunt, B.G.	1966	The photochemistry of ozone in a moist atmosphere, J.G.R., 71, 1385-1398. Also JATP, 23, 885.

Hohnson F.S., Purcell,	1954	Studies of ozone layer over New Mexico' in Rocket Exploration of the Upper Atmosphere, Ed. R. Boyd and M.J. Secton, p.189, Pergamon Press., London.
Kaufman, F.	1964	Aeronomic reactions involving hydrogen, a review of recent laboratory studies, Ann. Geophys., 20, pp.106-114.
Maeda, K.	1968	Ann. Geophys., 24, 1.
Mikirov, A.V.	1965	The estimation of ozone concentration at the heights of 44-102 Km during nights launching of geophysical rockets, Geom. Aeron., 5, 1120.
Miller, D.E. and Stewart, H.H.	1965	Observation of atmospheric ozone from an artificial earth satellite, Proc. Roy. Soc., A, 288, 540.
Nagata	1968	Space Research, VIII.
Pearce J.B.	1969	Rocket measurement of nitric oxide between 60 and 96 Km, JGR, 74, 853.
Randhawa J.S.	1968	Mesospheric ozone measurements during a solar eclipse, JGR, 73,(No.2),493.
Reeves, R.R.,Manella,G and Harteck P.	1960	Rate of recombination of oxygen atoms, J. Chem.Phys., 32, pp.632-633.
Smith, L.G.	1968	Ozone concentration at sunrise by absorption spectroscopy, Illinois Aeronomy Conf., p.89 (Tuesday).
Shimazaki, T.	1967	Dynamic effects on atomic and molecular oxygen density distributions in the upper atmosphere : a numerical solution to equations of motions and continuity, J.A.T.P.,29, 723.
Shimazaki,T and Laird, A.R.	1969	Dynamic effects of vertical distribution of minor neutral constituents in the Region 40 to 150 Km. (Correction to Illinois manuscript by Shimazaki).
Venkateswaran		Rocket and Satellite Meteorology, Ed. Wexler, pp.199-209.

Legends of Diagrams

Fig. 1 Observations on ozone distributions obtained by various workers with rocket and satellite-borne instruments.

Fig.2 Characteristic times for atomic oxygen (τ_1) and ozone (τ_3) computed by different workers. Hesstvedt's curves include oxygen-hydrogen reactions; the others for oxygen-only atmosphere.

Fig.3 Characteristic times for water vapour and various hydrogen components.

Fig.4 Diurnal variations of atomic oxygen and ozone computed by Maeda and Aikin (1967) for an oxygen-only atmosphere.

Fig.5 Latitude variations in ozone concentration computed by London (1967) compared with observational results.

Fig.6 Schematic diagram giving important reactions in the production and loss of atomic oxygen and ozone with current values of reaction rates.

Fig.7.a,b Height distributions of atomic oxygen production and loss rates for each reaction. Note that not all reactions are important. From these curves it is possible to select the dominant reactions for each height. Curves (a) are for daytime and curves (b) for night.

Fig.8.a,b Height distributions of ozone production and loss rates for each reaction. Note that not all reactions are important. From these curves it is possible to select the dominant reactions for each height. Curves (a) are for daytime and curves (b) for night.

Fig.9 Photochemical distributions of ozone obtained by different workers under different assumptions. Note the differences in the distributions. The distribution given by Shimazaki and Laird (private communication) is for an oxygen-hydrogen-nitrogen atmosphere.

Fig.10 Keneshea's computations on changes in ozone concentrations during the solar eclipse of November 12, 1966.

Fig.11 Variations in LF phase compared with changes in ozone concentrations during the solar eclipse of July 1963.

Fig.12 Negative ion scheme with current reaction rates.